Contents

List of Figures **5**

1 Estimation of seasonal variation in vulnerability and mortality in Dungeness Crab (*Cancer Magister*) **1**

1.1 Introduction . . . 1
1.2 Methods . . . 4
1.2.1 Population Dynamics . . . 4
1.2.2 Definition of Aggregation . . . 5
1.2.3 Assembly of Aggregations into Population . . . 11
1.2.4 Time Independent Vulnerability Hypotheses . . . 12
1.2.5 Time Dependent Vulnerability Hypotheses . . . 13
1.2.6 Negative Log-Likelihood . . . 16
1.2.7 Performance metrics . . . 17
1.2.8 Simulation Evaluation . . . 18
1.3 Results . . . 19
1.3.1 Likelihood Profiles . . . 20
1.3.2 Summary of Vulnerability . . . 30
1.3.3 Summary of Legal Biomass . . . 30
1.3.4 Summary of Exploitation Rate . . . 31
1.3.5 Performance Metrics . . . 31
1.3.6 Yield Per Recruit . . . 31
1.3.7 Simulation Evaluation . . . 32
1.4 Discussion . . . 32

Bibliography **51**

.1 Appendix . . . 52

List of Figures

1.1 Biological Events Flowchart: This flow chart shows how the biology of a single aggregation is advanced each week. The numbers in the nodes are relevant equations. . 6
1.2 Fishing Flowchart 9
1.3 Population Flowchart: This flowchart shows how a population of aggregations is advanced. The loop between advance biology and harvest an agent emphasizes that there are many aggregations that need to be updated. 13
1.4 Birth Weeks 22
1.5 Raw Temperature data from Buoy Station 46183 in the North Hecate Strait from the dates 05/15/1991 through 03/28/2017. 23
1.6 Average Weekly Temperature by week of year from Buoy Station 46183 in the North Hecate Strait, averaged across the dates 05/15/1991 through 03/28/2017 by week. (The average discards temperatures recorded that appear due to buoy malfunction.) 24
1.7 Negative Log-Likelihood 25
1.8 Error 36
1.9 Catch and Effort 37
1.10 Size Composition Fits 38
1.11 Vulnerability Comparison 39
1.12 Biomass Comparison 40
1.13 Moult Comparison 41
1.14 Exploitation Rate Comparison 42
1.15 Constant YPR 43
1.16 Variable YPR 44
1.17 Shell YPR 45
1.18 Effort YPR 46
1.19 Seasonal YPR 47
1.20 Temperature YPR 48

Chapter 1

Estimation of seasonal variation in vulnerability and mortality in Dungeness Crab (*Cancer Magister*)

1.1 Introduction

The relationship between catches, fishing activity (effort), and resource abundance is of fundamental concern to fisheries science. Often catches per unit effort are assumed to be proportional to abundance. However, it is known that this assumption may be violated in many ways. Fishing effort seldom conforms to the implied condition of being randomly distributed over the entire spatial range of the fish stock [15]. The average skill level in the active part of the fishing fleet can change as a function of abundance (often termed effort sorting) [15]. The accessibility to capture of the exploited stock, e.g. spatial distribution can change interannually or seasonally [9]. Developing an exhaustive list of all the ways the above assumption that catch rate remains proportional to abundance can be violated is less important than developing methods that can detect if it is violated and whether such violations will cause biases in estimates of the quantities that management may care about. This chapter investigates two assumptions made in the population dynamics model that was fitted to seasonal catch and effort data for the Area A Dungeness crab fishery in Chapter **??**, i.e., that the natural mortality rate parameter μ is known, and that the vulnerability remains constant

throughout the fishing season. To relax these assumptions the population dynamics model is fitted to the same weekly catch and effort data as before. Additionally, the size composition records from the Area A soft shell survey are also fitted. This chapter proposes some alternative mechanisms for how vulnerability may change within the fishing season, and characterizes each of them using parsimoniously parameterized models. By comparing the fits of these to the data, we can evaluate their relative plausibility.

This chapter investigates the following alternative notions about vulnerability and selectivity: soft shell crabs are subject to handling mortality, size selectivity operates for crabs in the soft shell condition (but all crabs in the catch are assumed to be fully selected at 165 mm), the vulnerability of crabs operates at the aggregation level, and the vulnerability of crabs operates at the population level.

There are often observed seasonal patterns in catch, effort, and abundance in fisheries [11, 19]; these patterns could be affected by systematic changes in the coefficient of catchability. Presume that the catchability coefficient q relates $CPUE$ (catch per unit effort) to biomass in the following way: $CPUE_t = q \cdot A_t$, $CPUE$ is the catch harvested in a single unit of fishing effort and abundance (A) is either in numbers of individuals or biomass [7]. If q changes over time it is possible to write $q_t = q \cdot \omega_t$ where ω_t is a time changing fraction applied to the catchability such that $CPUE_t = q\omega_t \cdot A_t$. It is conventional to scale the time-dependent fraction ω_t so that it is between zero and one and call the fraction the "vulnerability" or "selectivity". The language is somewhat confusing particularly since "vulnerability" is often viewed as the "probability of entering the gear" and "selectivity" is often viewed as the "probability of being retained by the gear" [7]. This thesis takes the pragmatic definition of "vulnerability" as the fraction ω_t.

While a detailed definition and contextualization of crab fishery vulnerability is best left to the methods, results, and discussion, the main point of this chapter is the evaluation of time changing patterns in the relationship between catch, effort, and abundance. Time-varying patterns in the relationship between catch, abundance, and effort may have management implications; for example, if Dungeness crabs are more vulnerable to harvest in some shell conditions, compared to other shell conditions, then there may be some weeks with a higher catchability than other weeks. Wise management may depend on setting the opening date of the fishery late enough to avoid setting

many traps on soft shell crabs (that cannot be marketed) while having the fishery open during the period of maximum vulnerability.

The two time-independent vulnerability hypotheses are as follows: first, all aggregations are fully vulnerable year around (this is the scenario in Chapter **??**), second, the relative vulnerability of a crab aggregation is uniformly distributed. The first time-independent vulnerability hypothesis serves as a base case against which to compare the other scenarios. The second time-independent vulnerability hypothesis models a population of crabs that consists of some crabs that are easier to catch than other crabs.

The time-dependent vulnerability hypotheses allows for vulnerability to change depending on: shell condition, time of year, the number of traps in the water, and the average weekly sea surface temperature in the Hecate Strait. While the precise definition of these hypotheses is best left for the methods section, it should be noted that the scenarios are consistent with the hypotheses advanced by industry and observed in other crustacean fisheries. For example, Ziegler et al. [19] studied the catchability of southern rock lobster as a function of water temperature, moulting, and mating. They found that water temperature changes were able to explain 62% of the variation in catchability and that moulting also was a notable driver of catchability. Also, McLeese and Wilder [9] found that the catchability of Atlantic lobster was linearly related to water temperature. While I am not aware of any empirical studies of seasonal variation of catchability in Dungeness crab fisheries, it is plausible that water temperature, moulting, and other things result in seasonal changes in catchability ($q \cdot \omega_t$). Several studies have been shown that water temperature is important in the timing of crustacean moulting [8, 11, 14], so there are good reasons for environmental signals to drive key crustacean behaviours.

Broadly there are five different (primary) ways to assess the abundance of a crustacean (or indeed any fish) stock: direct surveys [10], depletion methods [13], change in ratio methods [1], index removal methods [4], and tagging methods [4]. It is common to develop methods that compose these primary methods into a composite stock assessment. For example, statistical catch at age models typically include a combination of depletion and change in ratio methods [15].

By using size composition data, the model developed in this chapter effectively combines ideas from change in ratio estimators, since crabs less than $165mm$ are not harvested, with the depletion model developed in Chapter **??**. The size composition data from the soft shell survey is a time

series of data collected independently from the depletion time series. This chapter attempted to use the size composition data to learn about natural mortality, but it failed in that attempt. Since the size composition data is collected as part of the soft shell survey and uses traps that have their sub-legal crab escape rings closed, the size composition data should be more representative of the population than what would be available from sampling the catches.

Due to variation in available funds, the number of traps hauled in the soft shell survey varies across years. Since the soft shell survey is designed as a research survey without specific targeting of legal-sized hard-shell males, it is presumed that the sampled size composition data is representative.

1.2 Methods

The model developed in Chapter **??** is extended to include the different vulnerability hypotheses by changing Equation 1.7 which harvests crabs in an aggregation from $C_t = qE_tA_t$ to $C_t = qv_{a,t}E_tA_t$. Where $V_{a,t}$ is the relative vulnerability of the aggregation (not the total population) at time t. It should be noted that q has units crabs per unit effort; it is not biomass per unit effort since larger crabs contribute more biomass than smaller crabs. Since the size distribution changes under heavy fishing, this implies that more biomass per unit effort is harvested earlier in the season than later in the season. As a reminder, the equation in 1.7 is at the aggregation, not population level. It should be noted that $V_{a,t}$ is not constrained to be less than one when applied to individual aggregations. This is simply to make an estimation of the vulnerability parameter easier. It is always possible to re-scale the vulnerability and catchability such that at the population level the maximum vulnerability is one, as is conventional.

1.2.1 Population Dynamics

In the interest of completeness and making sure that the methodology of this chapter is capable of standing alone many of the methods in Chapter **??** are reproduced here. This chapter is an extension of the depletion Chapter **??** that changes relationship between catch, effort, and abundance. It also fits to the size composition data in the spring time.

1.2.2 Definition of Aggregation

A population of crabs in the model has variable moulting schedules and growth rates can be assembled from aggregations of crabs that have identical moult schedules and growth rates. In this subsection the dynamics of a single such aggregation is discussed; the assembly of these aggregations into a population is presented later.

The state of each aggregation is advanced one week using two separate routines for the biology and fishing dynamics. The population of crabs advances by updating the state of many different aggregations of crabs. These routines are applied to each aggregation each week.

Biological dynamics of a single aggregation

Figure 1.1 presents a flow chart for the routine that advances the biology of a single aggregation of crabs by a single week. A description of each node is presented below. Equations in this subsection apply only to a single aggregation. When presenting routines that advance a single aggregation the chapter does not use a subscript to denote which aggregation is being referenced. However, when the aggregations are assembled into a population, a subscript denoting aggregation is added.

1. Check if aggregation is alive. For the aggregation to be alive, the date in weeks must be greater than or equal to the birth-week of the aggregation. If the aggregation is alive go check if the aggregation changes shell condition, otherwise (it is dead) do nothing and return to the simulation.

2. Check if the aggregation changes shell condition. If the number of weeks in a shell condition is less than or equal to the duration of the shell conditions (see table Table 1.1), then the shell condition remains the same and the counter of the number of weeks in shell condition is incremented by one and natural mortality is applied. If the shell condition changes, then test if the crabs moult. While the order of shell conditions (5, 4, 3, 2, 1, 6, 8, 7) is non-intuitive, they follow the D.F.O. soft shell protocol [3]. When crabs leave shell condition 8, they moult into shell condition 5. If the number of moults exceeds the maximum number of moults (4 moults) then, instead of transitioning from shell condition 6 into shell condition 8, they transition into shell condition 7 (old shell) where they remain for the rest of their lives. The different shell conditions are shown in Table 1.2. Note that the sum of the durations in weeks, excluding

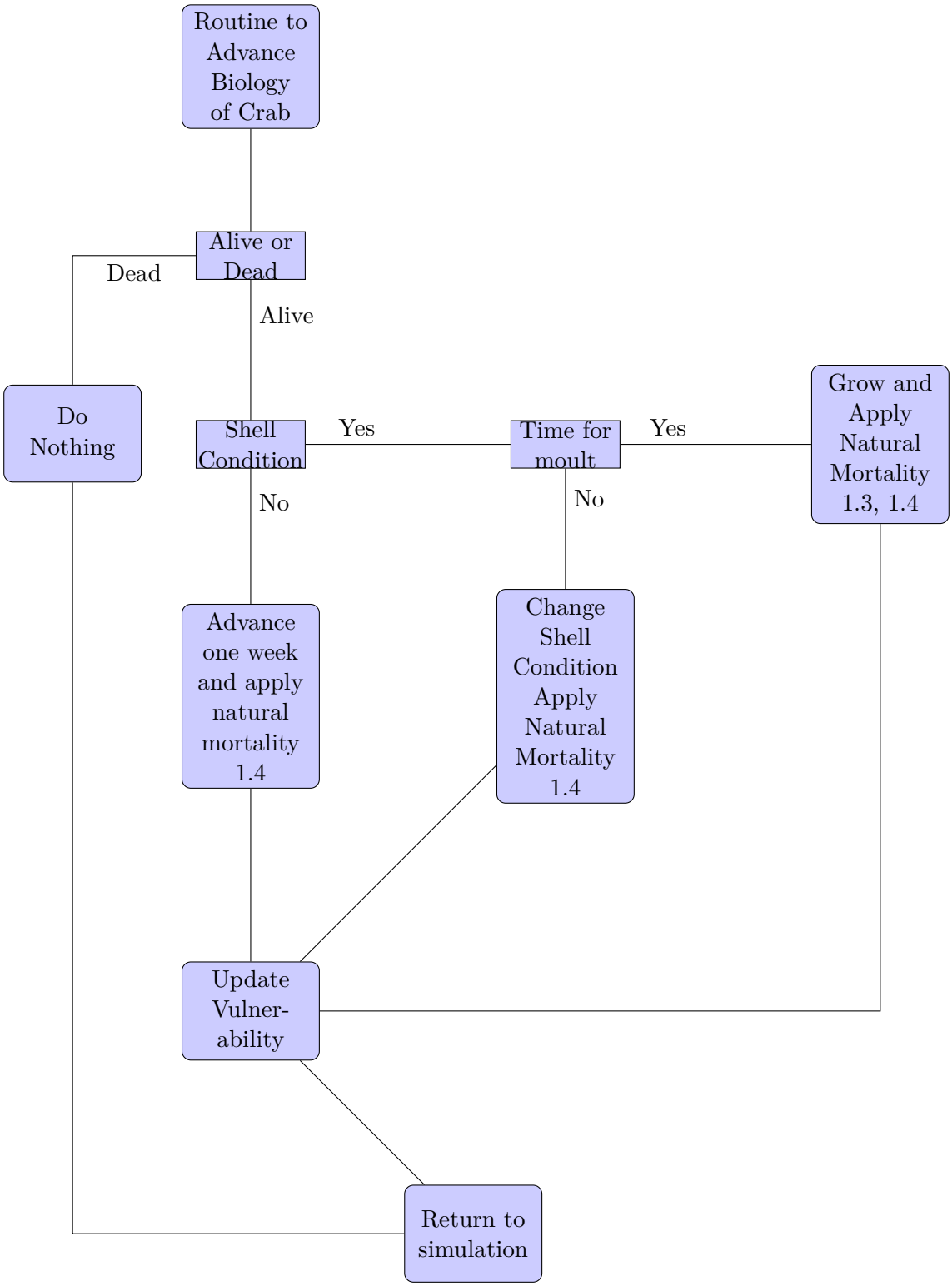

Figure 1.1: Biological Events Flowchart: This flow chart shows how the biology of a single aggregation is advanced each week. The numbers in the nodes are relevant equations.

shell condition 7, is 52. This is required since I assume crabs moult once a year, on a fixed schedule. (It is assumed there is no variability in the inter-moult period.) Crabs enter shell condition 1 and become legal to harvest 13 weeks after moulting.

Shell Condition	1	2	3	4	5	6	8	7
Duration in weeks	6	4	6	2	1	8	25	∞

Table 1.1: Shell Condition Duration Table in weeks

Shell Condition	Soft Shell Survey Definition	Time Since Moult	Code
Soft	Soft Just Moulted	2-6 Days	5 and 4
	Very New	6 Days - 1 Month	3
	New	1-3 Months	2
Hard	Newly hard	3-6 Months	1
	Between New and Old	6-12 Months	8
	Old	12-24 Months	6
	Very Old	More than 24 Months	7

Table 1.2: The hardness of crab shells determined by how much time has elapsed since the moult.

3. Check if aggregation moults. If crabs are transitioning from shell condition 8 into shell condition 5, then they moult. Otherwise advance the shell condition, apply natural mortality, and reset the counter on the number of weeks in a shell condition.

4. If crabs moult then they grow according to Equation 1.3, where L_{new} is the length of crabs in the aggregation after growing and L_{old} is the length of crabs in the aggregation prior to moulting. In Equation 1.3 the intercept is drawn as: $\beta \sim N(\mu = 18.07, \sigma = 3.29)$ when the aggregation is initialized, some aggregations grow faster than others. (Note there is no variability in the slope.) Once the aggregation's growth model intercept β is defined, it never changes. Each time an aggregation moults a counter is also incremented so that after a set number of moults (5 moults) crabs stop moulting and transition into shell condition 7. Unlike Zhang et al. [17], this model does not have size-dependent moulting probabilities; it assumes that crabs moult annually until they stop moulting, this may be an oversimplification. However, allowing crabs to moult or not moult would substantially increase the number of aggregations required to model the population; this is because some aggregations would have to skip moult, and the model would need to include aggregations that stopped moulting early. It is important to

remember that the week does not advance until the routine returns to the simulation; each equation is applied in sequence.

5. The weekly mortality depends on the shell condition of the aggregation. The weekly mortality rate is a function of the shell condition, this function is given in Equation 1.4, where A_t is the abundance in aggregation, M_{sc} is the relative weekly mortality for each shell condition, and μ scales the relative weekly mortalities. For the purposes of this chapter, μ is set to 10 as the default. In their annual model Zhang et al. [17] used both an instantaneous annual mortality ($M = .5$) and a post moult survival rate (70% survive). While it is not possible to estimate the mortality rate on each shell condition, it is clear that mortality is several-fold higher on soft shell crabs than hard shell crabs. Table 1.4 shows the assumed weekly relative natural mortality; these weekly relative mortalities were partially informed by the numbers in Zhang et al. [17]. Soft shell crabs should have much higher weekly mortality than hard shell crabs, but estimating the relative mortalities is probably impossible.

Fisheries dynamics on a single aggregation

Figure 1.2, presents a flow chart for the routine that conducts the fishery on a single aggregation.

1. Check if aggregation of crabs is alive. If the aggregation is alive go to check if the crab in the aggregation are legal, otherwise do nothing and return to the simulation.

2. Check if aggregation is legally available for harvest. The size and sex of the aggregation of crabs must be checked. If the aggregation is in soft shell condition three (not legal) apply the handling mortality Equation 1.7. If the aggregation is legal apply the harvest Equation 1.7.

3. Harvest the crabs if they are legal. To harvest the crabs commercially Equation 1.7 is applied. E_t is the total fishing effort. The parameter q is the catchability of a unit of effort. The possibly time varying vulnerability of the aggregation is expressed as v_t. In this chapter time varying vulnerability is considered. To convert from numbers of crabs harvested to mass of crabs harvested from an aggregation Equation 1.3 is used.

4. Apply handling mortality to non-legal crabs. The handling mortality routine only kills crabs in shell condition 3. This is based on comments that the Area A fisherman's association has

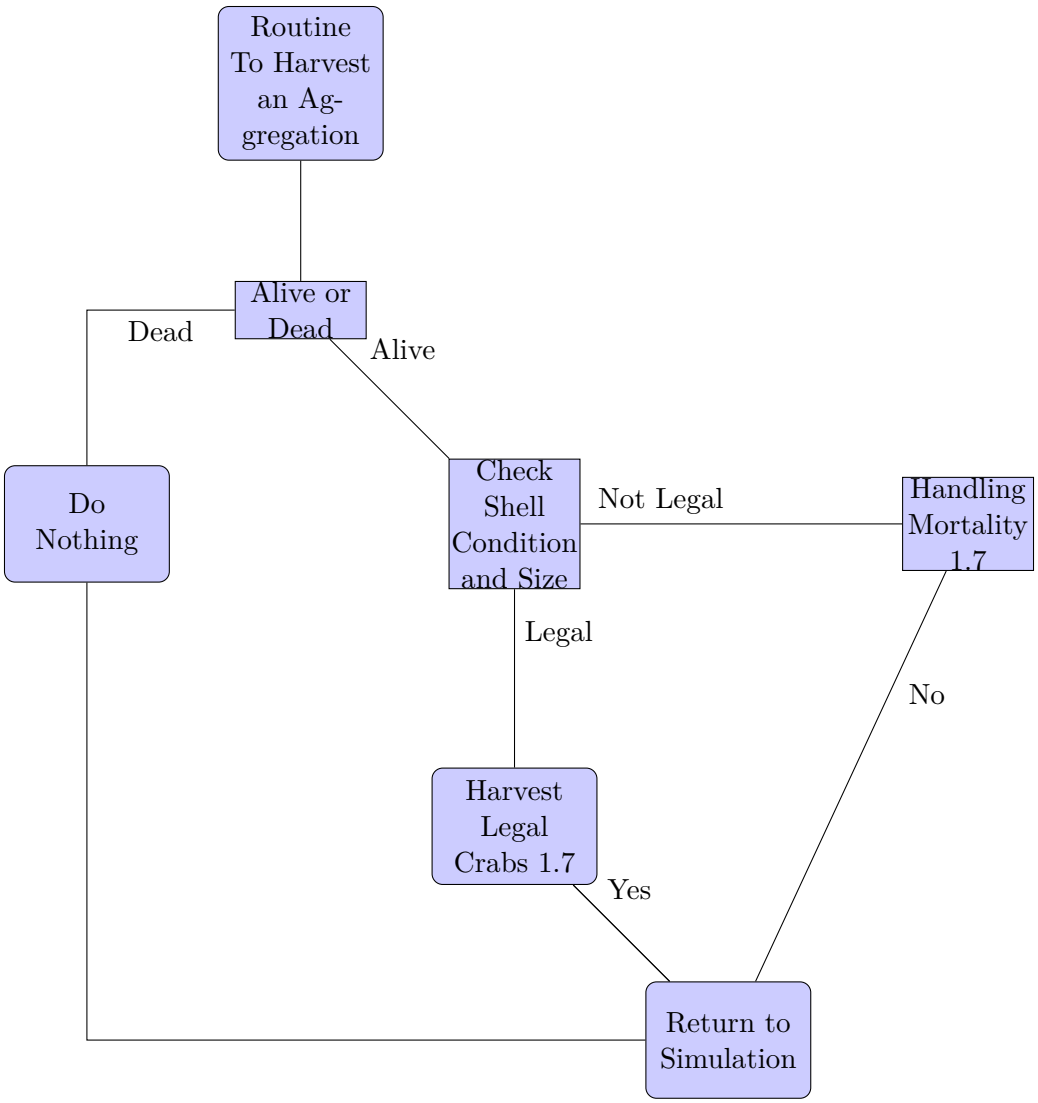

Figure 1.2: Fishing Flowchart: This flowchart shows how fishing is applied to each aggregation on a weekly time step. (SC is the shell condition.) The numbers in the nodes are relevant equations.

made; however it is likely that handling mortality may impact other shell conditions. If the crabs are in shell condition 3, handling mortality is implemented according to Equation 1.7, where the parameters are as in Equation 1.7. However, not all of the crabs that get caught are killed and none of the crabs that are caught contribute to the catch. The handling mortality constant M_h, was set at $.49wk^{-1}$ so that few crabs survive three captures in shell condition 3.

Symbol	Definition
L_{new}	Length after moult
L_{old}	Length before moult
α	Slope of linear growth model
β	Intercept of linear growth model (mm)
W	Mass in grams of crab at a given length
A_t	Abundance in aggregation at time t
A_{t_b}	Abundance in aggregation before applying relevant equation (the population is advanced one week only after all aggregations have been advanced)
A_{t_a}	Abundance in aggregation after applying relevant equation
A_t^T	Population abundance in aggregation at time t
A_t^a	Abundance in aggregation a at time t
μ	Mortality scalar on weekly mortality
M_{sc}	Weekly mortality by shell condition
C_t	catch in number of crabs in week t
q	catchability
E_t	Effort in week t
V_t	Vulnerability of an aggregation in time t. Note that $V_{a,t}$ is used when summing over aggregations.
M_h	Handling mortality fraction. Only applies if soft shell

Table 1.3: Table that defines symbols in equations

$$L_{new} = \alpha L_{old} + \beta \tag{1.1}$$

$$\alpha = 1.069 \tag{1.2}$$

$$\beta \sim N(\mu = 18.07mm, \sigma = 3.29)$$

$$W = .0001(L)^{3.0597} \tag{1.3}$$

$$A_{t_a} = A_{t_b}(1 - \mu M_{sc}) \tag{1.4}$$

$$C_t = q v_t E_t A_{t_b} \tag{1.5}$$

$$A_{t_a} = A_{t_b} - C_t \tag{1.6}$$

$$A_{t_a} = A_{t_b} - M_h q v_t E_t A_{t_b} \tag{1.7}$$

Shell Condition	1	2	3	4	5	6	8	7
Weekly mortality	.0005	.010	.015	.025	.05	.005	.005	.5

Table 1.4: Assumed weekly mortality by shell condition. Note that crabs only enter shell condition 7 after four moults and are assumed to be senescent.

1.2.3 Assembly of Aggregations into Population

The aggregations described above are assembled into a population according to rules described below. Each aggregation of crabs has a birth-week, that along with the moulting schedule, determines the shell condition of that aggregation of crabs in any week. A population of crabs is initialized by setting a regular pattern of birth-weeks for the decade prior to the first fishing season of interest; initializing the number of aggregations according to the pattern shown in Figure 1.4. Although most of the analyses undertaken used the variable pattern (shown in black) to drive the moult pattern, the constant moult pattern (shown in red) was also fit to data. The population is advanced by advancing each aggregation one week according to the routines shown in the previous section. (See 1.1 and 1.2). Each aggregation has its own growth rate, and depending on it's age and birth-week, will have a uniquely determined size and shell condition. By having more aggregations with birth-weeks in particular months, a main moulting period can be established. Figure 1.4 shows how many aggregations are initialized in each week as black and red points and a scaled line showing the proportional catches in 2003. The moult timing was assumed to be fixed; estimating the number of aggregations moulting in each week is infeasible. There are assumptions made about when crabs moult relative to the fishery's opening and the duration in shell conditions; for example,

in the model, aggregations moult every 52 weeks after they are initialized and the same number of aggregations is initialized each week of the year for every year. In week i of each year (where i is between 1 and 52) the same number of aggregations is initialized in each year. The initial abundance in each year is determined by estimating the abundance of the aggregations initialized in a single year; the abundance entering the model in week i is $N_y \cdot num(i)$ where N_y is the estimated abundance in a year and $num(i)$ is the number of aggregations born in week i. Equation 1.8 shows how to compute the total weekly catches, where TC_t is the total catch in kilograms in week t and $CM_{t,a}$ is the catch in kilograms removed from aggregation a at time t. (num_t is the number of living aggregations at time t.) Other quantities of interest can easily be computed in a similar fashion, for example, the total legal abundance can be computed by summing the legal abundance (1.9) at time t of all the living aggregations in week t. The legal abundance of an aggregation ($LA_{t,a}$) is the abundance in an aggregation if the aggregation is larger than 165 mm and in hard shell. The legal abundance is zero otherwise.

$$TC_t = \sum_{a_t=1}^{num_t} \frac{.0001 L_{old,a}^{3.0597}}{1000} \tag{1.8}$$

$$TLA_t = \sum_{a_t=1}^{num_t} LA_{t,a} \tag{1.9}$$

1.2.4 Time Independent Vulnerability Hypotheses

In Equation 1.7 each aggregation has a potentially time dependent vulnerability v_t that denotes it's vulnerability. For clarity, the vulnerabilities are denoted as $v_{a,t}$. For the time-independent vulnerability hypotheses, the relative vulnerability does not change over time. Since the vulnerability does not depend on time it can be written as v_a instead of $v_{a,t}$. The first time-independent vulnerability hypothesis assumes that all aggregations are equally vulnerable to harvest. This is the same hypothesis assumed in Chapter **??**, i.e. $v_a = 1$ for all aggregations. The second time-independent vulnerability hypothesis assumes that some aggregations are more vulnerable to fishing than oth-

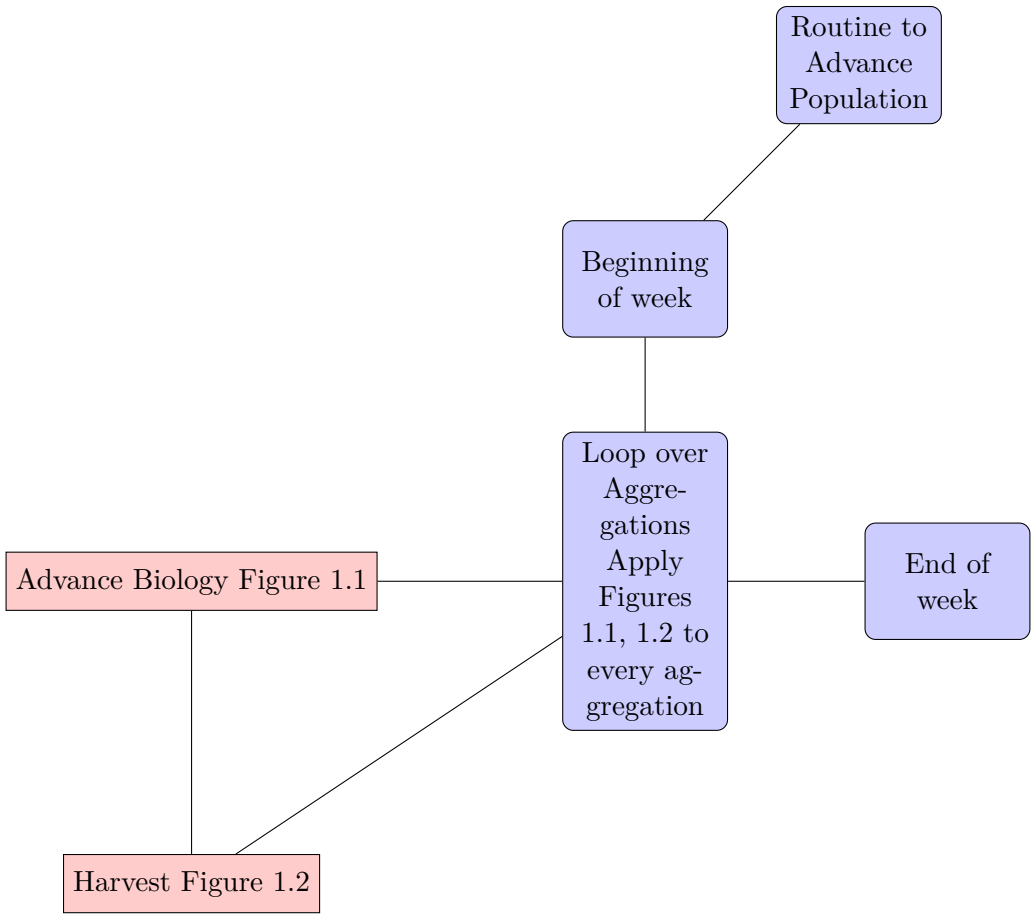

Figure 1.3: Population Flowchart: This flowchart shows how a population of aggregations is advanced. The loop between advance biology and harvest an agent emphasizes that there are many aggregations that need to be updated.

ers. The vulnerability was assumed to be uniformly distributed between $1-\alpha_v/2$ and $1+\alpha_v/2$ (with the mean vulnerability set to 1), where α_v an estimated parameter that defines an interval. However, for computation, we divided the interval into 10 bins of width $\frac{\alpha_v}{10}$ and computed a list of bins $s = 1-\alpha_v/2+\frac{\alpha_v}{10}\cdot v$ where v is a vector going from zero to 9. Then the vulnerability of each aggregation is set as $v_a = s[cid\%10]$. Where cid is a unique identification number for the aggregation and % is the modulo operator; thus every 10th aggregation has the same vulnerability and all bins are equally distributed through the population.

1.2.5 Time Dependent Vulnerability Hypotheses

The four time-dependent vulnerability hypotheses all require an additional parameter that changes the vulnerability over time. The first time-dependent vulnerability hypothesis depends on shell

Table 1.5: Opening and Closing Dates 2001-2014 (This table ignores minor variation in the opening and closing dates of some sub areas; the model is not spatial and treats the entire area as a unit.

Year	Open	Close	Open
2001	1-Jan	1-Mar	5-Jul
2002	1-Jan	4-Mar	5-Jul
2003	1-Jan	19-Apr	8-Jul
2004	1-Jan	19-Apr	2-Jul
2005	1-Jan	28-Apr	29-Jul
2006	1-Jan	Unknown (after 5-May)	26-Jul
2007	1-Jan	3-Apr	16-May
2008	1-Jan	22-Apr	16-Jul
2009	1-Jan	18-May	20-Jul
2010	1-Jan	19-Apr	15-Jun
2011	1-Jan	28-Feb	13-Jul
2012	1-Jan	13-May	30-Jun
2013	1-Jan	5-Jul	1-Aug
2014	1-Jan	1-Mar	23-May

condition (SC_a). If the shell condition is 1 (see Table 1.1 for a description of shell condition), the crabs have newly hardened shells, and they are fully vulnerable. If the shell condition is not 1, then the relative vulnerability is α_{sh}, where α_{sh} is an estimated parameter.

$$\begin{aligned} v_{a,t} &= 1 \text{ if } SC_a = 1 \\ v_{a,t} &= \alpha_{sh} \text{ if } SC_a \neq 1 \end{aligned} \tag{1.10}$$

The second time-dependent vulnerability hypothesis has crabs of all shell conditions being fully vulnerable between the 18th and 36th week of the year and have the relative vulnerability α_{se} the rest of the year. Note that these dates were chosen, somewhat arbitrarily, to separate the year into a summer and winter season.

$$\begin{aligned} v_{a,t} &= 1 \text{ if } 18 \leq t \leq 36 \\ v_{a,t} &= \alpha_{se} \text{ if otherwise} \end{aligned} \tag{1.11}$$

The effort dependent vulnerability hypothesis uses an exponentially weighted moving average of crabbing effort to compute a vulnerability weight; the vulnerability is the minimum of one and the vulnerability weight raised to the power of the vulnerability parameter α_e, where α_e is an estimated parameter. The exponential moving average, and the vulnerability, is computed as follows. The value of the decay of the moving average was chosen arbitrarily at 0.4. It should be noted that if $\alpha_e = 0$ it turns into the constant vulnerability scenario and depending on the sign of α_e vulnerability can either increase or decrease as a function of effort. The denominator was chosen so that VW_t was about equal to one during the peak of the harvest.

$$\begin{aligned} VW_{t+1} &= .4\frac{E_t}{40000} + (1-.4)VW_t \qquad (1.12) \\ v_{a,t} &= 1 \text{ if } VW_t^{\alpha_e} >= 1 \text{ otherwise} \\ v_{a,t} &= VW_t^{\alpha_e} \end{aligned}$$

The final time-dependent vulnerability model drove vulnerability as a linear function of the average weekly sea surface temperature. The sea surface temperature is recorded every few minutes by a buoy in the Hecate Strait. The buoy is Station 46183 in the North Hecate Strait and the data is available from NOAA online. (How to cite the Buoy?) Unfortunately, there are certain periods where the buoy reports implausible temperatures. For example, some recorded temperatures approached 100 degrees Celsius. In Figure 1.5 the chapter shows the raw data from 1995-2017 by timestamp. This shows that the seasonal temperatures are broadly the same across years and that there are periods where the buoy records non-sensible values. Figure 1.6 shows the average temperature, by week of year, after discarding any recorded temperature greater than 28 degrees Celsius or less than -4 degrees Celsius. This averaged temperature across the years is the weekly average temperature used in this analysis. The vulnerability is defined in Equation 1.13 where T is the average weekly temperature shown in Figure 1.6 and α_t is the slope of the line and like all αs is estimated to best fit the observations. T_{min} is the minimum weekly average temperature and T_w is the average weekly temperature in the week of year that t lines up with.

$$v_{a,t} = \alpha_t T_w + (1 - \alpha_t T_{min}) \tag{1.13}$$

$$T_{min} = 7.1323 \tag{1.14}$$

1.2.6 Negative Log-Likelihood

To incorporate the size composition data into the likelihood function I assume the following three things: 50% of the crabs are selected at $165mm$, there is logistic selectivity with the slope (ν) estimated as a nuisance parameter, and the scaled sample size is ten percent of the observed size composition sample to adjust for non-random sampling. To be clear the selectivity is only applied to the survey size composition, not the commercial catch. Using the size composition data allows me to try to estimate a scalar μ that scales the weekly natural mortality vector defined in Chapter **??**; unfortunately the data proved to be inadequate. To convert, between the model's predicted size composition ss_b in week of year 21, 22, 23, 24 (end of May early April) to crabs that would be selected s_b (in size bin b) we apply equation 1.15. W_{sample} is ten percent of the crabs sampled in the survey in a given year. S_i and $\hat{S}_i$ are the size composition that is predicted and observed in size class i. Aside from adding the size composition data to the likelihood, it is the same as in Chapter **??**.

$$s_b = \frac{1}{(1 + exp(\nu(-ss_b + 165))} \tag{1.15}$$

$$nll(x) = \sum_t^T -log(\frac{1}{\sigma\sqrt{2\pi}} e^{-\frac{(C_t - \hat{C}_t)^2}{2\sigma^2}}) - \sum_i^I S_i \cdot log(\hat{S}_i) W_{sample_i} \tag{1.16}$$

For each of the time-dependent vulnerability hypothesis a likelihood profile across the appropriate α is computed and a systematic comparison of the models, including computing the AIC, is undertaken. It should be noted that the vulnerabilities being computed in each of Equations 1.10, 1.11, 1.12, 1.13 are at the aggregation level, to scale up to the population level requires taking the average across aggregations and deciding if you want to account for soft shell crabs in this average

Title	Equation Number	Vulnerability Models and NLL	Terms
Shell	1.10	Shell condition	α_{sh} relative vulnerability of crabs not in shell condition 1
Season	1.11	Season	α_{se} relative vulnerability of crabs in winter
Effort	1.12	Bait in the water	α_e slope on smoothed weight
Temperature	1.13	Average water temperature	α_t Slope on smoothed temperature
NLL	1.16	Fits model to data	

Table 1.6: Summary of Equations, shown in text, that are used to set vulnerability models and fit to the data.

or not. In general, we treat soft shell crabs as not vulnerable. So in all models vulnerability declines during the moult. However, since the fishery is typically closed during the moult and soft shell crabs cannot legally be harvested the models have $E_t = 0$ when the aggregation is soft shell, $v_{a,t}$ can be anything since $0 = C_t = v_{a,t} A_t \cdot 0$.

The yield per recruit was computed in the same way as in Chapter **??**. I choose a default $M_h = .49wk^{-1}$ (see Equation 1.7) and ran the yield per recruit analysis for each of the vulnerability hypotheses.

1.2.7 Performance metrics

The percent handling loss is computed the same way that it is computed in the yield per recruit analysis, except that it is computed using the estimated abundance and is not at equilibrium (see Equation 1.17. Where NH_t is the weekly catch without handling mortality and H_t is the weekly catch with handling mortality.

$$H_t = \sum_t^T \frac{NH_t - H_t}{H_t} \tag{1.17}$$

The depletion is computed as the minimum of the total number of legal-sized males divided by the total number of legal-sized males there would be without fishing each year. For the metric, we take the average for each year as shown in Equation 1.18, where $D1$ is the depletion in 2003, $D2$ is the depletion in 2004, etc. LA_t is the legal abundance in week t of the appropriate year and $LA_{t,nf}$ is the legal abundance that would be present without fishing in week t of the appropriate year. Depletion is computed using numbers of animals, not biomass.

$$
\begin{aligned}
D1 &= min\left(\frac{LA_t}{LA_{t,nf}}\right) \\
D2 &= min\left(\frac{LA_t}{LA_{t,nf}}\right) \\
D3 &= min\left(\frac{LA_t}{LA_{t,nf}}\right) \\
D4 &= min\left(\frac{LA_t}{LA_{t,nf}}\right) \\
D5 &= min\left(\frac{LA_t}{LA_{t,nf}}\right) \\
D_{total} &= \frac{D1+D2+D3+D4+D5}{5}
\end{aligned} \tag{1.18}
$$

Fishing mortality is computed as in Equation 1.19, where C_t is the numbers, not biomass, of crabs caught in week t and LA_t is the legal abundance. Legal abundance is crabs larger than $165mm$ regardless of their shell condition.

$$
F = -\sum_{t}^{T} log(1-(C_t/LA_t)) \tag{1.19}
$$

1.2.8 Simulation Evaluation

To evaluate if the estimates in catch and legal abundance are biased, both the total bias and the root mean square error of the differences between simulated and estimated catches are computed. This chapter simulates several data sets under one vulnerability model and estimates the parameters under another vulnerability model. However, since the vulnerability models are often different studying the bias in the parameters is not particularly useful. Instead, this chapter compares the bias in weekly catch, exploitation rate, and legal abundance (Equation 1.20) and the root mean square error in catch and legal abundance (Equation 1.21). Where $Vsim$ and $Vest$ are the simulated and estimated values of weekly catch, exploitation rate, or legal abundance T is the maximum

number of weeks, and t is the weekly index.

$$bias = \frac{1}{T}\frac{\sum_t^T V_t^{est} - V_t^{sim}}{\bar{V_t^{sim}}} \tag{1.20}$$

$$RMSE = \frac{1}{T}\frac{\sqrt{\sum_t^T (V_t^{est} - V_t^{sim})^2}}{\bar{V_t^{sim}}} \tag{1.21}$$

As in Chapter **??** the simulated data has 5% observation error added to it as in Equation 1.22. The chapter used the estimated parameters and the estimated covariance matrix to draw the simulated parameters for each of the vulnerability hypotheses from a multivariate normal distribution. These are the same metrics shown in Chapter **??** Equation **??**.

$$RC_j \quad \sim \quad N(C_j, .05C_j) \tag{1.22}$$

1.3 Results

There are four different types of results presented for this chapter. The first involves looking at the likelihood profiles of the different time-dependent vulnerability hypotheses and comparing them to the likelihood values from the time-independent vulnerability hypotheses. The second concerns best fit under the different vulnerability hypotheses. The third is a yield per recruit analysis comparing yield per recruit across the different vulnerability hypotheses. The fourth concerns simulation evaluation analyses. This chapter revealed that trying to estimate natural mortality μ was very difficult. The appendix shows that failed attempt, in particular many non-diagonal elements in the correlation matrices were 1. This chapter's results are shown assuming that μ is equal to 10, note that μ is multiplied by the weekly natural mortality vector shown in Table **??**.

1.3.1 Likelihood Profiles

Any time-dependent vulnerability hypotheses needs to offer substantial improvements to the fit for it to be worth the extra parameter. It should be noted that there exist some values of α for each vulnerability hypothesis such that the vulnerability hypothesis reduces to the constant vulnerability hypothesis. Under the variable, temperature, and effort vulnerability hypotheses the model becomes the constant vulnerability hypothesis when α is equal to zero. The seasonal vulnerability hypothesis becomes the constant vulnerability hypothesis when α is equal to one. In Table 1.7, I show the number of parameters, NLL, AIC, and the depletion and size composition components of the deviance. Most of the difference between the scenarios is in how well they fit the observed catches.

All of the time-dependent vulnerability hypotheses had lower AIC's than the time-independent vulnerability hypotheses. Furthermore, it should be noted that the best-fitting vulnerability hypotheses were the temperature and shell condition hypotheses. This is consistent with several other crustacean fisheries [14].

In Figures 1.7, I show the negative log-likelihood profile as a function of the parameter α for each of the vulnerability hypothesis. The horizontal line is 1.92 units above the minimum and indicates the confidence intervals, although there are some modest discrepancies between the confidence intervals from the Hessian (shown in red) and from the log-likelihood profile.

Just as in Chapter **??** the model was fit to two different moulting patterns. One where the crabs moult over a several week period and the other where all the crabs moult in a single week. Almost all the results are only shown for case where the crabs moult over several weeks. However, Tables 19, 1.11 and 1.13 show the results for the constant moult scenario. It is interesting that the depletion and fishing mortality estimates are not credible for the constant moult variable vulnerability scenario. (The variable moult variable vulnerability scenario is believable.) However, many of the other estimates are comparable between the constant moult and variable moult scenarios.

Vulnerability	Number of Parameters	NLL	Catch Component	Size Component	AIC	Δ AIC
Constant	7	7857	6039	1817	15728	128
Var	8	7854	6033	1820	15724	122
Seasonal	8	7834	6018	1816	15684	82
Effort	8	7825	6007	1818	15666	64
Shell	8	7816	5998	1819	15648	46
Temperature	8	7793	5979	1814	15602	0

Table 1.7: This table shows the scenario, the number of parameters, and the associated AIC. The scenario with the lowest AIC was the temperature dependent vulnerability scenario.

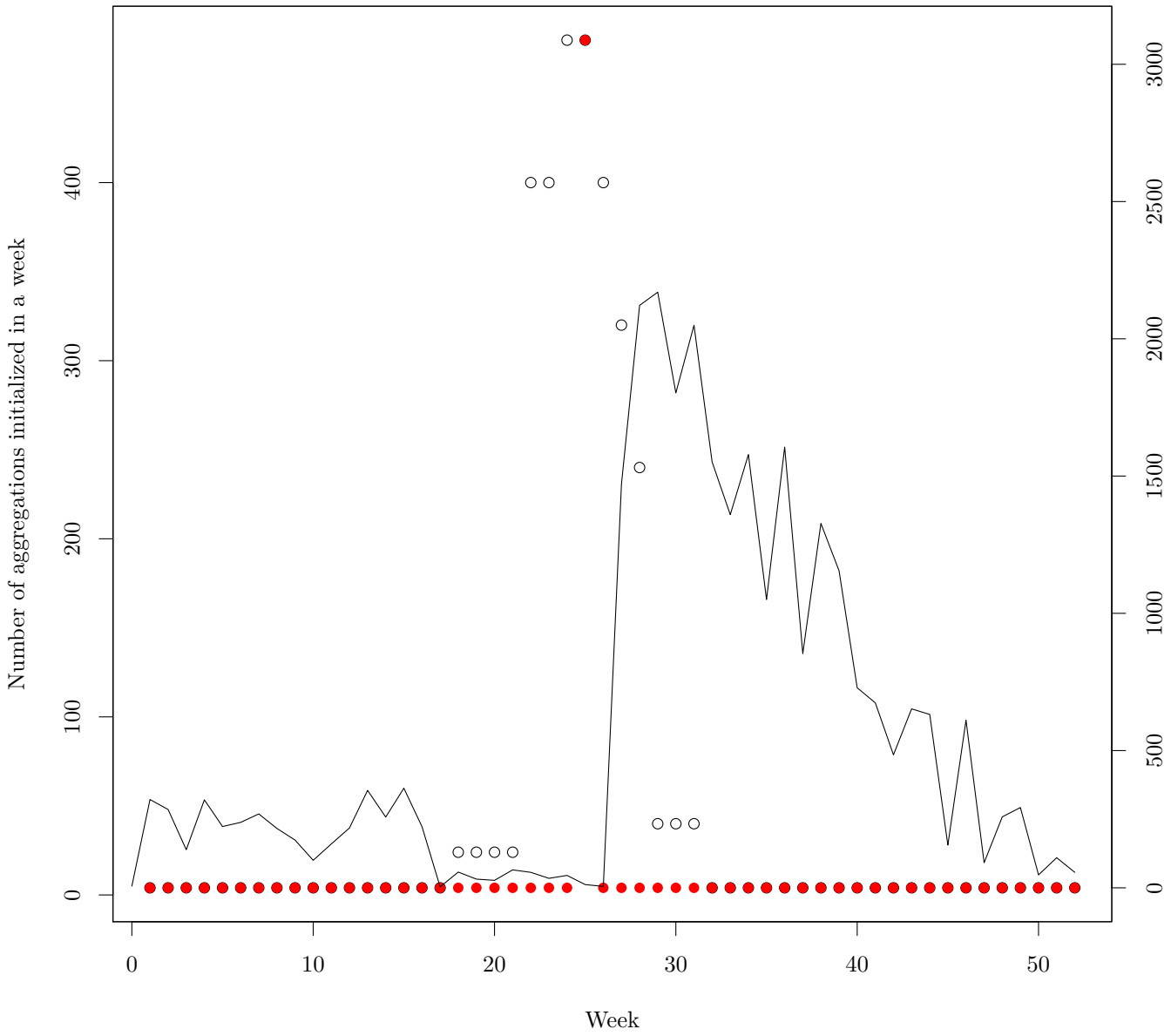

Figure 1.4: The dots show the number of aggregations born in each week. The black dots (left axis) are for the variable moult schedule, and the red dots (right axis) are for the constant moult schedule. The line shows the relative effort pattern in 2003 for reference; the crab moult several weeks prior to the fishery.

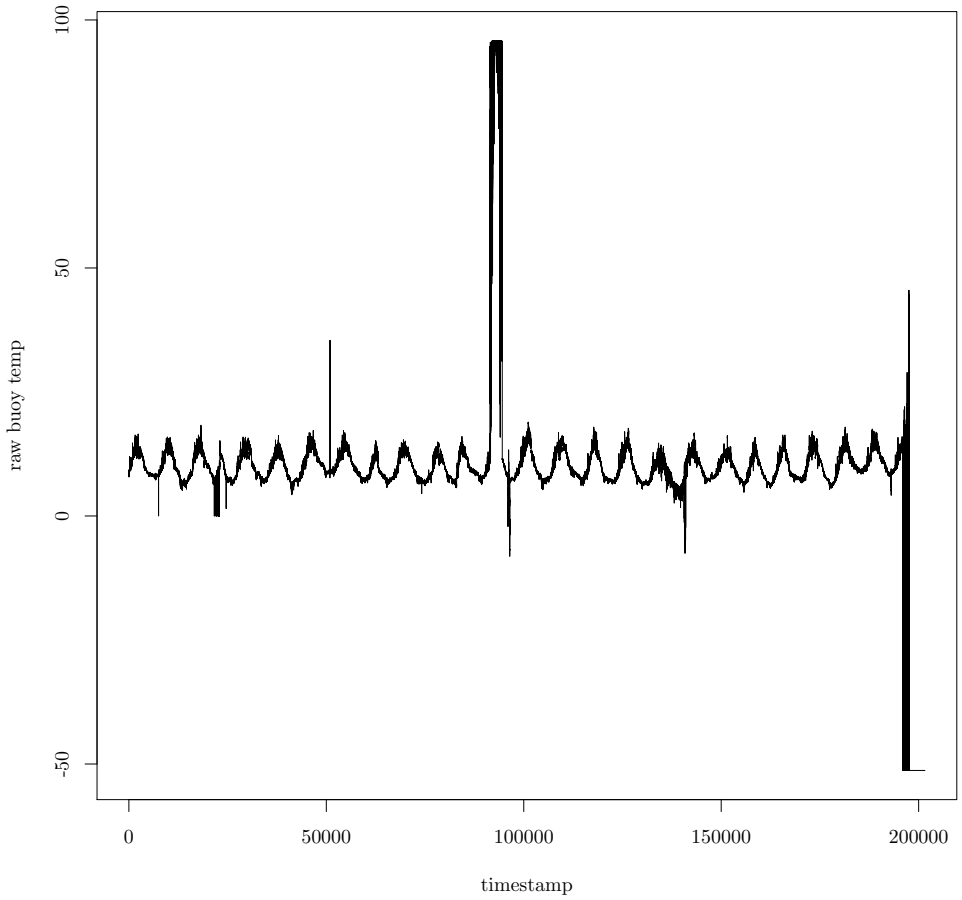

Figure 1.5: Raw Temperature data from Buoy Station 46183 in the North Hecate Strait from the dates 05/15/1991 through 03/28/2017.

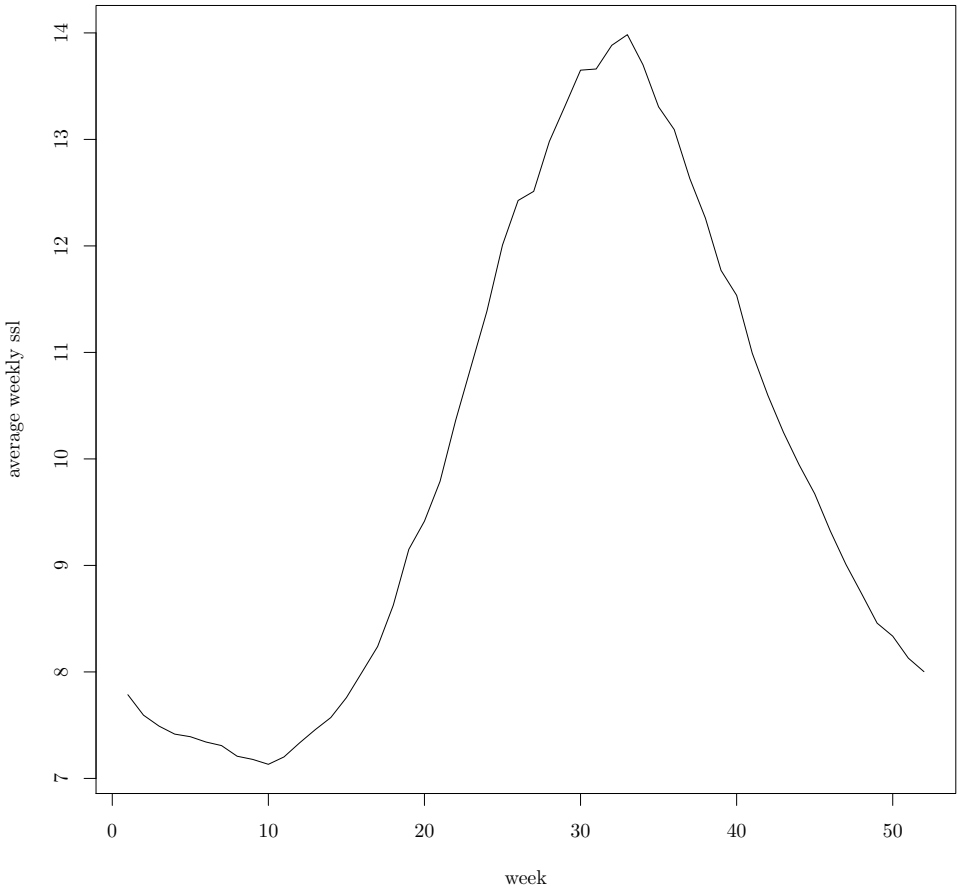

Figure 1.6: Average Weekly Temperature by week of year from Buoy Station 46183 in the North Hecate Strait, averaged across the dates 05/15/1991 through 03/28/2017 by week. (The average discards temperatures recorded that appear due to buoy malfunction.)

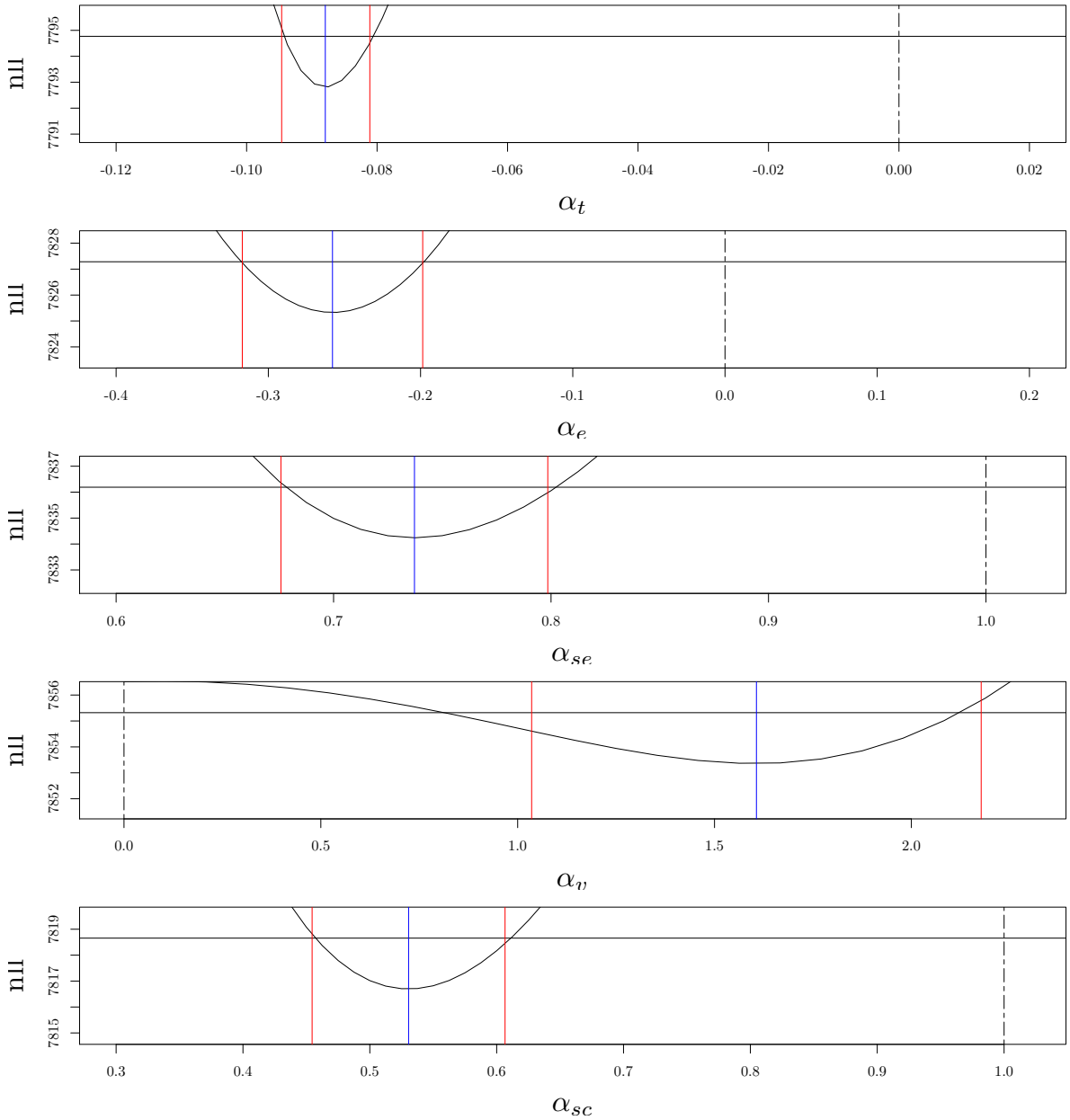

Figure 1.7: These figures present the negative log-likelihood profiles for the α parameter in each of the vulnerability hypotheses. The panels show results from top to bottom: temperature, effort, seasonal, variable, and, shell condition hypotheses. The red and blue vertical lines are the MLE and confidence intervals from the gradient search and the Hessian. The black dotted vertical line is the value of α that makes the vulnerability hypothesis equivalent to the constant vulnerability hypothesis.

	Const	Var	Shell	Seasonal	Effort	Temp
N1	0.4, 0.42, 0.45	0.41, 0.49, 0.56	0.52, 0.67, 0.91	0.41, 0.43, 0.44	0.45, 0.48, 0.51	0.5, 0.54, 0.57
N2	0.56, 0.6, 0.63	0.61, 0.68, 0.77	0.78, 1, 1.4	0.56, 0.58, 0.6	0.64, 0.68, 0.73	0.66, 0.68, 0.72
N3	0.29, 0.32, 0.34	0.32, 0.37, 0.42	0.52, 0.74, 1.1	0.27, 0.29, 0.31	0.33, 0.36, 0.39	0.33, 0.34, 0.36
N4	0.094, 0.12, 0.14	0.11, 0.13, 0.17	0.18, 0.28, 0.43	0.088, 0.1, 0.13	0.1, 0.13, 0.15	0.1, 0.12, 0.14
N5	0.35, 0.38, 0.4	0.38, 0.43, 0.49	0.52, 0.69, 0.96	0.34, 0.35, 0.37	0.41, 0.43, 0.46	0.38, 0.4, 0.42
q	1.6, 1.8, 1.9	2.7, 3, 3.4	0.72, 1.1, 1.4	2.4, 2.8, 3.3	1.5, 1.6, 1.7	4.1, 4.7, 5.3
ν	0.16, 0.17, 0.18	0.16, 0.17, 0.18	0.16, 0.17, 0.19	0.16, 0.17, 0.19	0.16, 0.17, 0.18	0.16, 0.17, 0.19
α	1, 1, 1	1.1, 1.6, 2.2	0.47, 0.54, 0.6	0.66, 0.73, 0.79	-0.31, -0.25, -0.2	-0.095, -0.088, -0.08

Table 1.8: Parameter estimates and 95% confidence intervals for the estimated parameters N_1, N_2, N_3, N_4, N_5, q, ν, and α under different vulnerability scenarios (Lower CI, Mean, Upper CI%). The confidence intervals are estimated using draws from a multivariate normal using the estimated covariance matrix and maximum likelihood estimates.

	Const	Var	Shell	Seasonal	Effort	Temp
N1	0.26, 0.46, 0.87	0.43, 0.47, 0.51	0.42, 0.46, 0.51	0.4, 0.42, 0.44	0.44, 0.47, 0.5	0.47, 0.49, 0.52
N2	0.37, 0.66, 1.2	0.62, 0.67, 0.73	0.62, 0.68, 0.75	0.56, 0.57, 0.59	0.63, 0.67, 0.72	0.62, 0.65, 0.68
N3	0.19, 0.36, 0.71	0.34, 0.36, 0.4	0.37, 0.42, 0.49	0.28, 0.29, 0.32	0.33, 0.36, 0.4	0.32, 0.33, 0.35
N4	0.064, 0.13, 0.25	0.11, 0.13, 0.17	0.12, 0.15, 0.19	0.083, 0.1, 0.12	0.1, 0.12, 0.15	0.1, 0.11, 0.13
N5	0.24, 0.43, 0.8	0.4, 0.43, 0.47	0.41, 0.45, 0.5	0.34, 0.36, 0.37	0.41, 0.44, 0.47	0.38, 0.4, 0.42
q	1.5, 1.7, 1.8	0.015, 0.27, 0.82	1.2, 1.4, 1.6	2.2, 2.6, 3	1.4, 1.5, 1.7	3.6, 4.1, 4.7
ν	0.16, 0.17, 0.19	0.16, 0.17, 0.19	0.16, 0.17, 0.19	0.16, 0.17, 0.19	0.16, 0.17, 0.18	0.16, 0.17, 0.19
α	1, 1, 1	-2.2, -1.8, -1.5	0.78, 0.83, 0.87	0.69, 0.75, 0.82	-0.3, -0.24, -0.19	-0.093, -0.084, -0.076

Table 1.9: Parameter estimates and 95% confidence intervals for the estimated parameters N_1, N_2, N_3, N_4, N_5, q, ν and α under different vulnerability scenarios under constant moult (Lower CI, Mean, Upper CI). Confidence intervals are estimated using the draws from a multivariate normal using the estimated covariance matrix and maximum likelihood estimates.

	Const	Var	Shell	Seasonal	Effort	Temp
Fishing Mortality	6.2, 6.8, 7.4	4, 5.2, 6.3	1.5, 2.5, 3.5	8.4, 9.6, 11	5.1, 5.7, 6.2	11, 12, 13
Percent Lost	0.17, 0.18, 0.2	0.17, 0.19, 0.21	0.033, 0.057, 0.082	0.25, 0.3, 0.35	0.15, 0.17, 0.18	0.43, 0.51, 0.59
Average Depletion	0.26, 0.29, 0.32	0.31, 0.38, 0.46	0.52, 0.62, 0.74	0.15, 0.18, 0.22	0.32, 0.35, 0.39	0.12, 0.14, 0.16

Table 1.10: Estimated metrics and 95% confidence intervals for the different vulnerability scenarios (Lower CI, Mean, Upper CI). Parameters are estimated using the draws from a multivariate normal using the estimated covariance matrix and maximum likelihood estimates.

	Const	Var	Shell	Seasonal	Effort	Temp
Fishing Mortality	5.3, 5.8, 6.3	10, 1, 28	3.5, 4.5, 7.8	7, 7.9, 8.8	4.3, 4.8, 5.3	8.1, 8.8, 9.7
Percent Lost	0.16, 0.17, 0.19	-0.37, 0.18, 0.69	0.095, 0.11, 0.14	0.24, 0.29, 0.33	0.14, 0.16, 0.17	0.37, 0.44, 0.52
Average Depletion	0.24, 0.27, 0.3	0.073, 0.27, 0.37	0.34, 0.4, 0.46	0.14, 0.17, 0.21	0.3, 0.33, 0.37	0.11, 0.13, 0.16

Table 1.11: Estimated metrics and 95% confidence intervals for the different vulnerability scenarios with constant moult (Lower CI, Mean, Upper CI). Parameters are estimated using the draws from a multivariate normal using the estimated covariance matrix and maximum likelihood estimates. Note that it appears to be impossible to estimate fishing mortality for the Variable vulnerability model. However, the average depletions are comparable between the constant and variable moulting schedules.

	Const	Var	Shell	Seasonal	Effort	Temp
Depletion 2003	0.25, 0.28, 0.31	0.3, 0.37, 0.45	0.5, 0.61, 0.73	0.15, 0.18, 0.22	0.31, 0.34, 0.38	0.12, 0.14, 0.16
Depletion 2004	0.23, 0.26, 0.29	0.28, 0.35, 0.44	0.49, 0.6, 0.73	0.13, 0.16, 0.19	0.29, 0.32, 0.36	0.1, 0.12, 0.14
Depletion 2005	0.23, 0.26, 0.29	0.28, 0.35, 0.44	0.49, 0.6, 0.73	0.13, 0.16, 0.19	0.29, 0.32, 0.36	0.1, 0.12, 0.14
Depletion 2006	0.31, 0.35, 0.38	0.36, 0.43, 0.5	0.6, 0.7, 0.8	0.18, 0.22, 0.26	0.37, 0.4, 0.44	0.14, 0.17, 0.19
Depletion 2007	0.26, 0.29, 0.32	0.31, 0.38, 0.46	0.51, 0.62, 0.74	0.16, 0.19, 0.22	0.33, 0.36, 0.4	0.14, 0.16, 0.18

Table 1.12: Depletion and 95% confidence intervals for the different scenarios (Lower CI, Mean, Upper CI). Parameters are estimated using the draws from a multivariate normal using the estimated covariance matrix and maximum likelihood estimates.

	Const	Var	Shell	Seasonal	Effort	Temp
Depletion 2003	0.23, 0.26, 0.29	0.07, 0.26, 0.37	0.33, 0.39, 0.45	0.14, 0.17, 0.21	0.29, 0.33, 0.37	0.089, 0.12, 0.15
Depletion 2004	0.22, 0.25, 0.28	0.065, 0.25, 0.36	0.31, 0.37, 0.43	0.13, 0.15, 0.19	0.28, 0.31, 0.35	0.096, 0.12, 0.14
Depletion 2005	0.21, 0.24, 0.27	0.063, 0.24, 0.35	0.31, 0.36, 0.43	0.11, 0.14, 0.18	0.27, 0.3, 0.34	0.087, 0.11, 0.13
Depletion 2006	0.29, 0.33, 0.36	0.09, 0.31, 0.42	0.41, 0.47, 0.53	0.16, 0.2, 0.25	0.35, 0.38, 0.42	0.13, 0.16, 0.18
Depletion 2007	0.24, 0.28, 0.31	0.074, 0.27, 0.38	0.34, 0.4, 0.46	0.15, 0.18, 0.22	0.31, 0.35, 0.39	0.14, 0.16, 0.18

Table 1.13: Depletion and 95% confidence intervals for the different scenarios with constant moult (Lower CI, Mean, Upper CI). Parameters are estimated using the draws from a multivariate normal using the estimated covariance matrix and maximum likelihood estimates.

	Const	Var	Effort	Seasonal	Shell	Temp
N1	0.40, 0.42, 0.45	0.42, 0.49, 0.57	0.45, 0.48, 0.51	0.41, 0.43, 0.45	0.50, 0.67, 0.91	0.50, 0.53, 0.57
N2	0.56, 0.59, .62	0.60, 0.69, 0.80	0.64, 0.68, 0.72	0.56, 0.58, 0.60	0.76, 1.00, 1.40	0.65, 0.68, 0.71
N3	0.29, 0.32, 0.34	0.31, 0.37, 0.43	0.33, 0.36, 0.39	0.27, 0.29, 0.31	0.50, 0.75, 1.10	0.32, 0.34, 0.36
N4	0.09, 0.11, 0.14	0.10, 0.13, 0.17	0.11, 0.13, 0.15	0.09, 0.10, 0.12	0.18, 0.28, 0.43	0.10, 0.12, 0.14
N5	0.35, 0.37, 0.40	0.37, 0.43, 0.50	0.40, 0.43, 0.46	0.34, 0.35, 0.37	0.50, 0.69, 0.96	0.38, 0.39, 0.41
q	1.6, 1.8, 1.9	2.70, 3.00, 3.40	1.5, 1.6, 1.7	2.40, 2.80, 3.20	0.73, 1.00, 1.40	4.10, 4.60, 5.30
ν	0.16, 0.17, 0.16	0.17, 0.19, 0.18	0.16, 0.17, 0.19	0.16, 0.17, 0.19	0.16, 0.17, 0.18	0.16, 0.17, 0.19
α	1, 1, 1	1.0, 1.6, 2.20	-0.20, -0.26, -0.32	0.67, 0.74, 0.80	0.45, 0.53, 0.61	-0.08, -0.083, -0.10

Table 1.14: Parameter estimates and 95% confidence intervals for the estimated parameters N_1, N_2, N_3, N_4, N_5, q, ν and α different vulnerability scenarios (Lower CI, Mean, Upper CI%). Parameters are estimated using the Hessian.

Const	N1	N2	N3	N4	N5	q	s
N1	1.00	0.45	0.36	0.14	0.43	-0.56	-0.15
N2	0.45	1.00	0.51	0.20	0.63	-0.81	0.05
N3	0.36	0.51	1.00	0.12	0.51	-0.66	0.04
N4	0.14	0.20	0.12	1.00	0.17	-0.26	-0.00
N5	0.43	0.63	0.51	0.17	1.00	-0.78	0.00
q	-0.56	-0.81	-0.66	-0.26	-0.78	1.00	-0.00
s	-0.15	0.05	0.04	-0.00	0.00	-0.00	1.00

Shell	N1	N2	N3	N4	N5	q	s	α_{sh}
N1	1.00	0.99	0.98	0.92	0.98	-0.99	0.05	-0.88
N2	0.99	1.00	0.98	0.93	0.99	-0.99	0.08	-0.89
N3	0.98	0.98	1.00	0.92	0.98	-0.98	0.08	-0.92
N4	0.92	0.93	0.92	1.00	0.92	-0.92	0.07	-0.86
N5	0.98	0.99	0.98	0.92	1.00	-0.99	0.07	-0.89
q	-0.99	-0.99	-0.98	-0.92	-0.99	1.00	-0.07	0.86
ν	0.05	0.08	0.08	0.07	0.07	-0.07	1.00	-0.08
α_{sh}	-0.88	-0.89	-0.92	-0.86	-0.89	0.86	-0.08	1.00

Effort	N1	N2	N3	N4	N5	q	s	α_e
N1	1.00	0.67	0.57	0.25	0.66	-0.70	-0.11	-0.46
N2	0.67	1.00	0.68	0.30	0.80	-0.86	0.03	-0.50
N3	0.57	0.68	1.00	0.22	0.68	-0.76	0.02	-0.35
N4	0.25	0.30	0.22	1.00	0.28	-0.34	-0.00	-0.14
N5	0.66	0.80	0.68	0.28	1.00	-0.85	-0.00	-0.47
q	-0.70	-0.86	-0.76	-0.34	-0.85	1.00	0.00	0.28
ν	-0.11	0.03	0.02	-0.00	-0.00	0.00	1.00	0.01
α_e	-0.46	-0.50	-0.35	-0.14	-0.47	0.28	0.01	1.00

Var	N1	N2	N3	N4	N5	q	s	α_v
N1	1.00	0.92	0.87	0.56	0.91	0.31	-0.11	0.91
N2	0.92	1.00	0.90	0.58	0.95	0.27	-0.03	0.93
N3	0.87	0.90	1.00	0.53	0.90	0.19	-0.03	0.86
N4	0.56	0.58	0.53	1.00	0.56	0.13	-0.03	0.55
N5	0.91	0.95	0.90	0.56	1.00	0.23	-0.05	0.91
q	0.31	0.27	0.19	0.13	0.23	1.00	-0.04	0.56
s	-0.11	-0.03	-0.03	-0.03	-0.05	-0.04	1.00	-0.06
α_v	0.91	0.93	0.86	0.55	0.91	0.56	-0.06	1.00

Season	N1	N2	N3	N4	N5	q	s	α_{se}
N1	1.00	0.15	0.02	-0.01	0.09	0.13	-0.15	-0.26
N2	0.15	1.00	0.20	0.07	0.33	-0.22	0.06	-0.03
N3	0.02	0.20	1.00	0.04	0.32	-0.47	0.03	0.33
N4	-0.01	0.07	0.04	1.00	0.07	-0.18	-0.00	0.13
N5	0.09	0.33	0.32	0.07	1.00	-0.46	-0.00	0.23
q	0.13	-0.22	-0.47	-0.18	-0.46	1.00	0.01	-0.91
ν	-0.15	0.06	0.03	-0.00	-0.00	0.01	1.00	-0.01
α_{se}	-0.26	-0.03	0.33	0.13	0.23	-0.91	-0.01	1.00

Temp	N1	N2	N3	N4	N5	q	s	α_t
N1	1.00	0.60	0.28	0.07	0.32	0.73	-0.07	-0.78
N2	0.60	1.00	0.31	0.10	0.41	0.64	0.06	-0.77
N3	0.28	0.31	1.00	-0.00	0.27	0.23	0.04	-0.36
N4	0.07	0.10	-0.00	1.00	0.04	0.05	0.00	-0.09
N5	0.32	0.41	0.27	0.04	1.00	0.22	0.01	-0.41
q	0.73	0.64	0.23	0.05	0.22	1.00	0.02	-0.93
ν	-0.07	0.06	0.04	0.00	0.01	0.02	1.00	-0.02
α_t	-0.78	-0.77	-0.36	-0.09	-0.41	-0.93	-0.02	1.00

Table 1.15: Parameter correlation matrix for the different vulnerability hypothesis. The vulnerability hypothesis is in the upper left corner. Note that the abundance is strongly correlated with natural mortality. Also, note that q and α are often strongly correlated. These covariance matrices are estimated from the Hessian.

Since the catchabilities q are multiplied by the vulnerabilities $V_{a,t}$ the estimated catchabilities are not directly comparable. It is not surprising that the estimates of α are somewhat inconsistent between the gradient and profile likelihood results since several of the parameters are strongly correlated. However, the differences are modest and both suggest that α is quite different from the value that would be equivalent to the constant vulnerability hypothesis.

In Figures 1.8, 1.9, and 1.10 I show the model fits to the observed catch and size composition data for each of the hypotheses. It is interesting to note that there are several places where there is a visibly better fit for one of the time-dependent vulnerability hypotheses compared to the constant vulnerability hypothesis. For example, the temperature vulnerability hypothesis better predicted the observed catches from June through September in 2004 and September through December in 2005. Also, the shell condition hypothesis visibly better fits the catch data September and October 2006. Finally, the temperature hypothesis fit better than the shell condition hypothesis in July 2004 and June 2007. This is consistent with the AIC calculations.

The best-fitting model used sea surface temperature to drive the vulnerability. The temperature vulnerability hypothesis fits the catch data better than the constant vulnerability hypothesis in many places. In contrast to the other vulnerability hypotheses, there were fewer legal males at the end of the fishing season than under the constant vulnerability hypothesis.

1.3.2 Summary of Vulnerability

In Figure 1.11, I show how the population level vulnerability changes throughout the season. As discussed in the methods, taking the weighted average of the aggregation vulnerabilities is needed to represent the vulnerability of the population. I include soft-shell crabs as crabs that are completely invulnerable to harvest in computing these vulnerabilities; hence the period of very low vulnerability when crabs moult in the model. To conform to convention, these averages have been re-scaled to lie between zero and one.

1.3.3 Summary of Legal Biomass

In Figure 1.12 I show how the biomass of legal-sized males changes throughout the fishing season. In all scenarios, the abundance of legal males appears to level off in November.

1.3.4 Summary of Exploitation Rate

In Figure 1.14 I show how the exploitation rate of legal males changes throughout the fishing season. It should be noted that a 2% weekly exploitation rate in July will result in a much higher catch than a 2% weekly exploitation rate in November since the legal abundance is lower in November.

1.3.5 Performance Metrics

The performance metrics for each of the different vulnerability hypotheses are shown in table 1.10 and the annual depletion is shown in Table 1.12. It should be noted that the depletion varied across the different vulnerability hypotheses. For example; about 35% of the crab was left under the constant, variable, and effort scenarios, but 65% was left under the shell vulnerability scenario, and only $15\% - 20\%$ was left under the seasonal and temperature scenarios.

1.3.6 Yield Per Recruit

In Figures 1.15, 1.16, 1.17, 1.18, 1.19, and 1.20 I show how, under the assumption that M_h is $.49wk^{-1}$, the yield per recruit and instantaneous handling mortality (f_{hsc3}) changes as a function of the effort scale and catchability for each of the six vulnerability hypotheses. The maximum yield per recruit is between about 240 and 700 grams, depending on the hypothesis. According to Zhang et al. [18], the moult survival rate was .7, and they found that the yield per recruit was between 100 and 300 grams. It is difficult to compare yield per recruit directly since crabs were recruited to the model (not the fishery) at 130mm in their model (versus 100mm in this chapter). Since handling mortality of sub-legal males is a major concern, including sub-legal males in calculating yield per recruit is important. In the plots, the vertical and horizontal lines show where the estimated catchability intersects the effort scale set at one. When the effort scale is two, there is twice as much effort as when the effort scale is one. It is interesting to note that neither the catchability nor the amount of effort is set directly by management; there are limits on the number of vessels in the fishery and trap design restrictions. We take the effort pattern and recruitment from the year 2003 for the yield per recruit since the model only makes sense when being forced with recruitment and weekly effort. The model does not have a non-zero equilibrium.

1.3.7 Simulation Evaluation

In Table 1.16, I show the results of the simulation evaluations. The first column denotes the vulnerability hypothesis of the simulated data, the second column denotes the vulnerability hypothesis assumed in the estimation model. It is reassuring, that I was able to recover true simulated values for catches and abundances with relatively little bias. The biases were mostly within plus or minus 10% in most cases when the correct vulnerability hypothesis was simulated and there was 5% observation error. However, there appears to be some moderate errors for the variable vulnerability model in the estimated abundances and estimated weekly exploitation rates. It is also clear that some large errors in estimates of abundance and exploitation rates can occur when an incorrect vulnerability model is assumed especially for the seasonal and temperature-based vulnerability models. The display of catch bias is important because it shows the model fits. The weekly exploitation rate is computed as catch mass divided by legal abundance biomass, not numbers.

A few points of interest are that under the case where the vulnerability hypothesis was both simulated and estimated there appears to be notable bias in legal abundance. It is also worth pointing out that these are time series and if the simulated values in a week are close to zero the biases could become quite large, or have some numeric instability since a very small number divided by a very small number can be far from one. I suspect that that is responsible for some of the very large values when the shell vulnerability hypothesis is simulated.

1.4 Discussion

Under all vulnerability hypotheses, a substantial amount of legal crab remains in the water after the fishing season. However, under the temperature-dependent vulnerability model, fewer legal males were left in the water than under the constant vulnerability model. This highlights how different structural assumptions about seasonal vulnerability patterns imply different exploitation rates. That said, no scenarios showed more than about a 70% decline in legal male abundance in 2004 (a high abundance year) and a 50% decline in 2006 (a low abundance year). The limited decline in abundance shows two things: that there is a limit to how severely the fleet can deplete legal abundance, undersize sex and season management. The percent decline in legal abundance is higher in high abundance years than in low abundance years. These results may have implications for the ongoing discussion about bringing valuable effort controlled fisheries in line with the pre-

cautionary approach. Interestingly a recent study of depletion of Dungeness crab was undertaken by Richerson et al. [12]. They found that the fisheries removed between 9% and 98% of the legal males. On average, the fishery removed 66% of the legal male population in Washington, Oregon, and California. Comparisons of different studies are difficult because different models make different assumptions about natural mortality and vulnerability. It is interesting that Richerson et al. [12] also concluded that a substantial amount of male crab remained in the water. Unfortunately, there do not seem to be any direct public estimates of post-harvest legal abundance. All depletion models must make assumptions about growth, natural mortality, and vulnerability. Perhaps it would be informative to use a bottom trawl survey or other non-depletion based method to cross-validate and better estimate natural mortality and time changes in vulnerability [2].

It is noteworthy that the weekly exploitation rate is quite different between the different vulnerability hypotheses. The different exploitation rates imply different legal abundances and different average instantaneous fishing mortalities between the different vulnerability hypotheses. The biggest differences are early in the fishing season. When comparing the fishing mortalities, remember that they are averaged over the entire year. The differences in weekly exploitation rates are much lower between December and May than June through September. Regardless of the vulnerability hypothesis getting the opening date right is likely to much more important to the fishery than getting the closing date right. The consequence of being closed between December and May is less important than being open as soon as the crab's shells harden post moult.

All of the time-dependent vulnerability hypotheses performed better than the constant and variable vulnerability hypotheses. Also, none of the confidence intervals of the σ parameters overlapped the value of σ that would make the vulnerability hypothesis equivalent to the constant vulnerability hypothesis, suggesting that assuming constant vulnerability is an oversimplification. However, three different mechanisms could be responsible for the changes in vulnerability. First, there could be effort sorting in the fleet. Early in the season, the fleet might be on average either less or more capable than later in the season, capable meaning not just fisher skill but heterogeneity in vessel size [16]. However, Chapter **??** did not find much evidence of effort sorting. This chapter does not keep track of how long a given trap was soaking in the water. It is unknown if soak times change as the season progresses. Perhaps effort sorting manifests in soak times rather than trap hauls. This chapter does not identify trap hauls by vessel or estimate a unique catchability for each vessel. It

cannot evaluate how cumulative harvest is distributed across the fleet. Second, there are spatial distribution questions. Private GPS data shows that effort is typically concentrated in a particular area early in the fishing season. As the season progresses, effort spreads out over a larger area. Since traps are on strings, the spatial location of a trap is not independent of other traps. This chapter does not look at the search behaviour of the fleet. Finally, the biology and behaviour of crabs may drive the changes in catchability. Ziegler et al. [19] found that water temperature was able to explain 62% of the variation in catchability. McLeese and Wilder [9] found that temperature is linearly related to the catchability of Atlantic lobster. Interestingly, the slope estimated in this chapter's temperature model is negative; crabs are most vulnerable in the winter. It seems that in other crustacean fisheries, catchability increased with water temperature. For example, McLeese and Wilder [9] found that lobster walked more in warmer water and catchability was proportional to walking. However, it is not surprising that environmental factors may affect catchability [6].

The time-dependent vulnerability hypotheses structurally imply that there was a shift in vulnerability between summer and winter. For example, since the water is warmer in the summer than the winter the temperature vulnerability model implies that either crabs are more vulnerable in the summer than the winter or vice versa. It is unclear if increasing the degrees of freedom would lead to a better understanding of temporal variation in vulnerability. The four seasonal models divide the year into periods of high and low vulnerability in similar ways. Having size composition data at the end of the season would enhance any model-based study of vulnerability. With size composition data at the end of the season, it may be easier to disentangle assumptions about growth, shell condition, natural mortality, and seasonal shifts in vulnerability. It is difficult to offer more than speculation about this. A few ideas come to mind, sea surface temperature may vary more dramatically than bottom temperature, and the sea surface temperature may act as a proxy for some other driver.

A legitimate concern is that the dates set for the opening and closing dates and the weights for the moving average in the effort model were somewhat arbitrarily chosen. Also, the structural assumptions made in all of the different time-dependent vulnerability hypotheses could be wrong. Perhaps it would be worthwhile to increase the number of parameters considered to include the dates that delineate the summer and winter season in the seasonal vulnerability model. Furthermore,

the weights on the moving average for the effort vulnerability model possibly could be estimated. However, strong assumptions are needed to create any model that can be fit to observations.

Crabs in the Hecate strait are not balls in an urn. Any depletion model must somehow define a function f that relates fishing effort, abundance, and catch. We often assume that $C_t = f(E_t, A_t) = qE_tA_t$ even though we have no good reason to believe catch is directly proportional to the product of effort and abundance. Hyperstability and hyperdepletion are common enough concerns as to be in textbooks [15]. As shown in the simulation evaluation table, simulating under one effort hypothesis and estimating under another was able to fit the catch series quite well even though there was some bias in the legal abundance. Given the paucity of data, this chapter cannot reliably estimate seasonal behaviour of the function f; however, it does highlight some of the open questions in the assessment of the crab stock. We had to make assumptions not only about f, but also moult timing, natural mortality, and growth. This chapter does not evaluate different combinations of vulnerability hypotheses. It lacked reliable size composition data after the bulk of the fishing season (but before the main moult). The most defensible conclusion is that the relationship between effort, catch, and abundance changes throughout the season.

The analyses in this chapter do not study the business drivers of the within-season dynamics of the fishery. However, the existing management regime allows for the unrestricted harvest of legal males during the summer. The existing management regime allows fishermen to exploit their observations and maximize their benefits. While the fishery remains open, the amount of fishing effort that the fleet deploys in a week is determined by harvesters' professional discretion. There is a growing consensus that managing fish stocks, conserving the marine environment, protecting fishermen's livelihoods, and protecting supply chains are complementary, not competing goals [5]. Grafton et al. [5] argues that finding ways to harmonize the individual incentives of harvesters with the fishery's overall objectives can be more successful than regulatory approaches that constrain fishermen in ways contrary to their perceived self-interest.

Clearly not all weeks are equally valuable to the fishery. Catchability and legal abundance changes over time. While considerable uncertainty remains about the above function f, vulnerability is not likely to remain constant over the season.

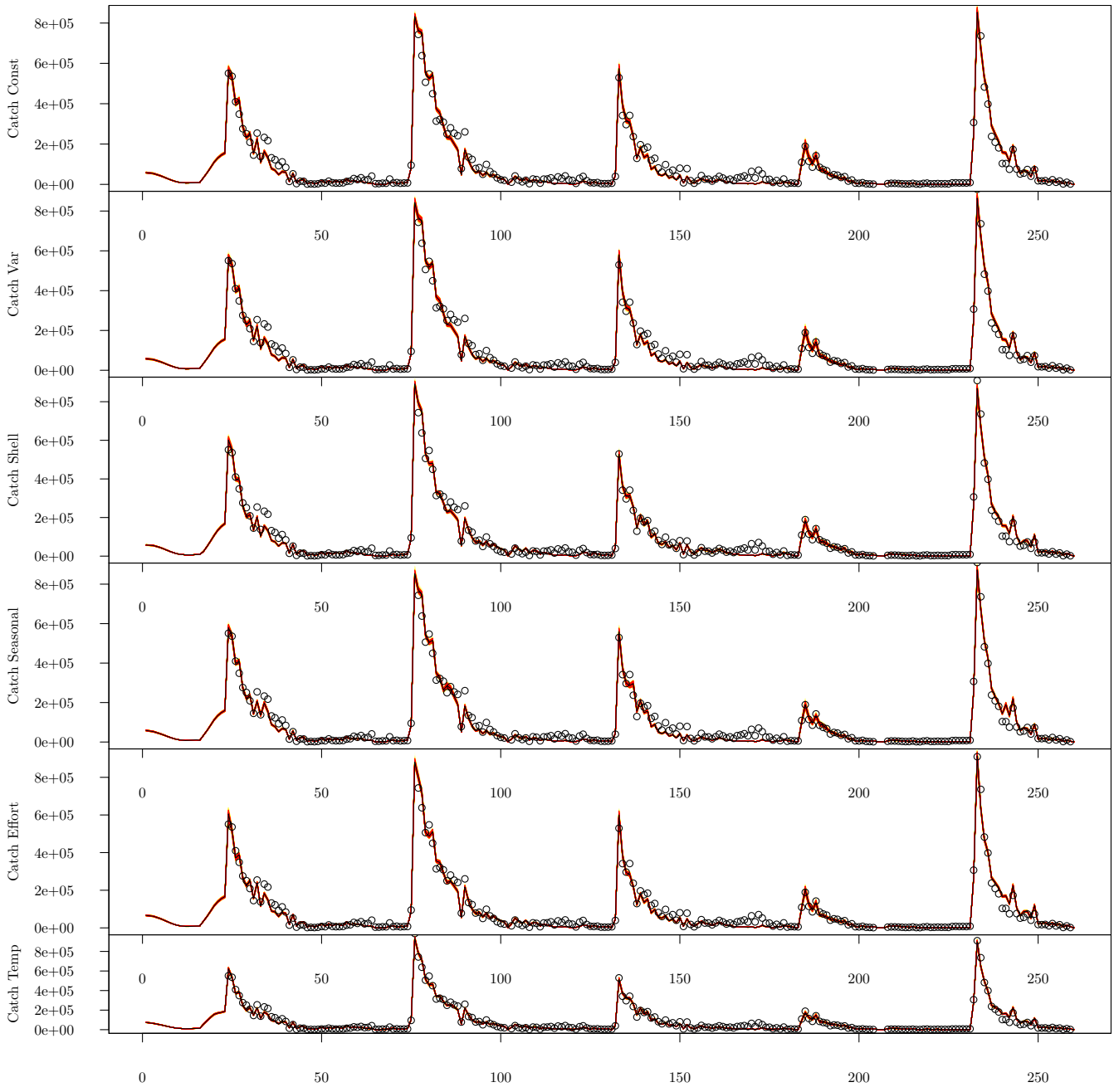

Figure 1.8: Fit to weekly catch records under the six vulnerability models. Catches are in Kilograms. This shows the entire time-series, subsequent plots select just a high and low abundance year.

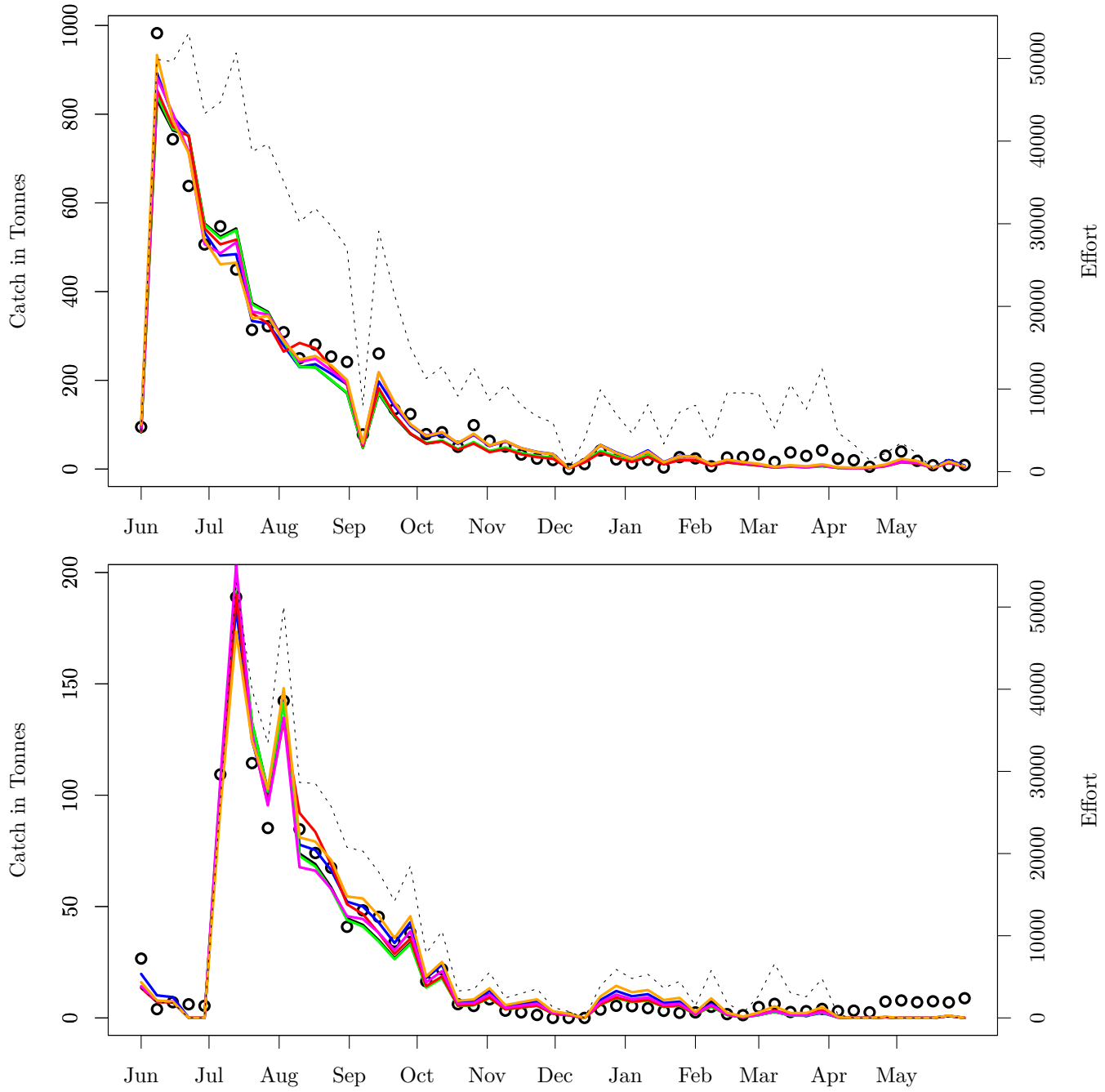

Figure 1.9: Catch and Effort: On the left y-axis I show the observed catches in tonnes(dots), and predicted catch in tonnes (solid line). On the right y-axis I show the number of traps hauled (dashed lines). The years are, from top to bottom, 2004, and 2006. The constant, shell, variable, seasonal, effort, temperature driven vulnerability hypotheses are shown in black, blue, green, red, magenta, and orange respectively.

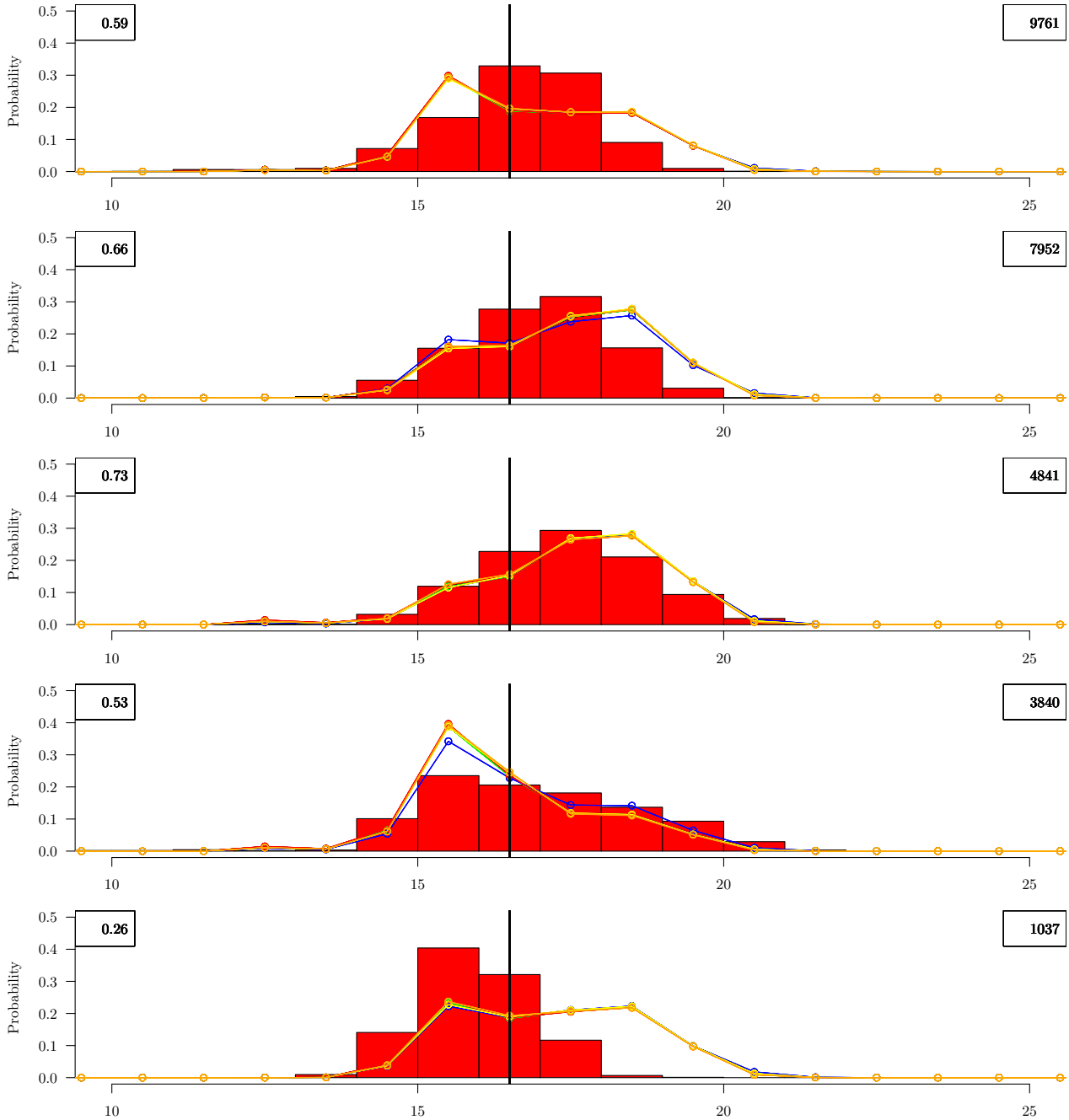

Figure 1.10: Size Composition Fits. On the left y-axis shows the proportions at size, the x-axis shows the size of crabs in millimetres. The years are, from top to bottom 2004, 2006. The constant, shell, variable, seasonal, effort, temperature driven vulnerability hypotheses are shown in black, blue, green, red, magenta, and orange respectively.

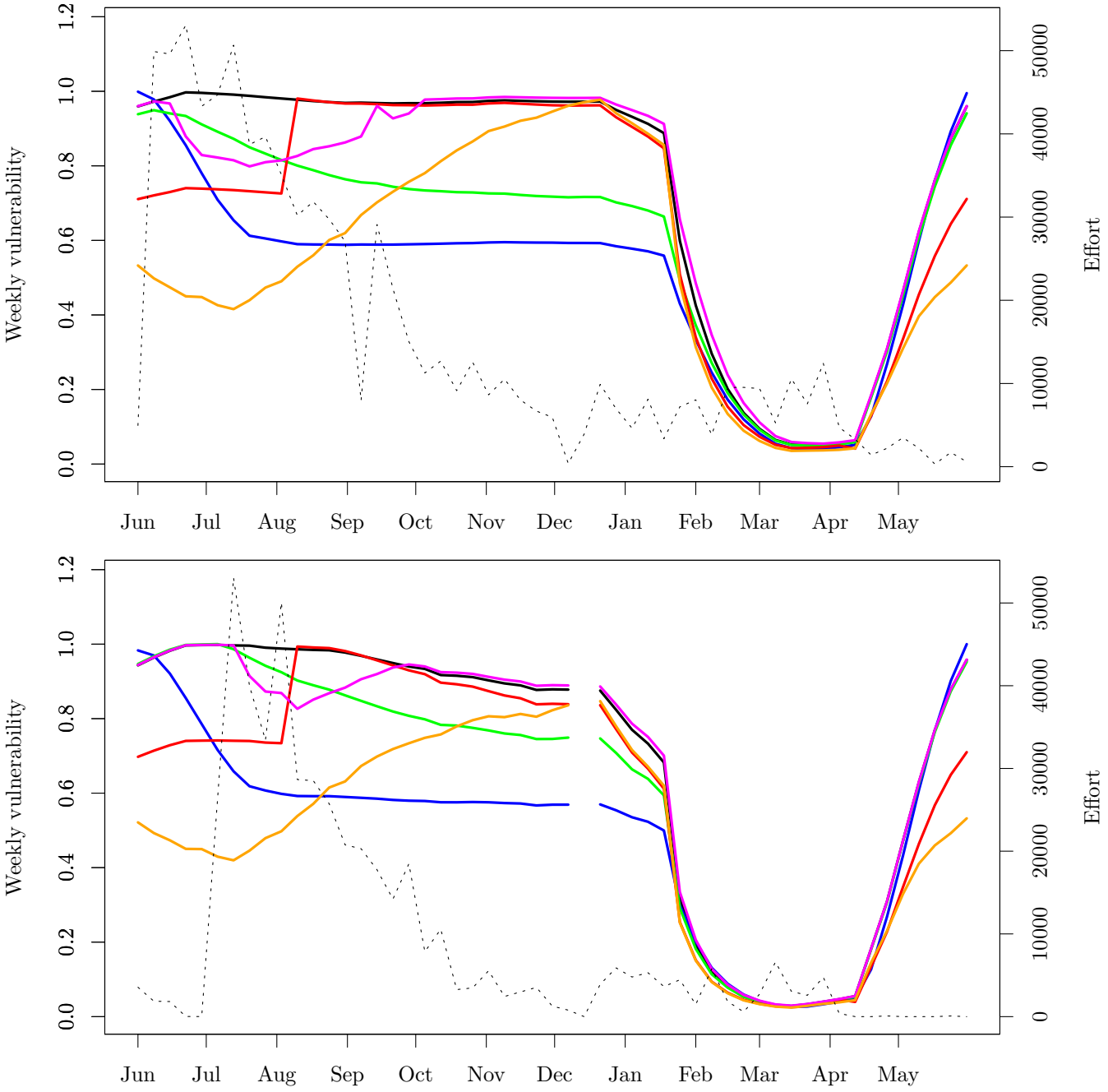

Figure 1.11: Vulnerability comparison. The years are, from top to bottom, 2004, and 2006. The constant, shell, variable, seasonal, effort, temperature driven vulnerability hypotheses are shown in black, blue, green, red, magenta, and orange respectively. On the right y-axis I show the number of traps hauled (dashed lines).

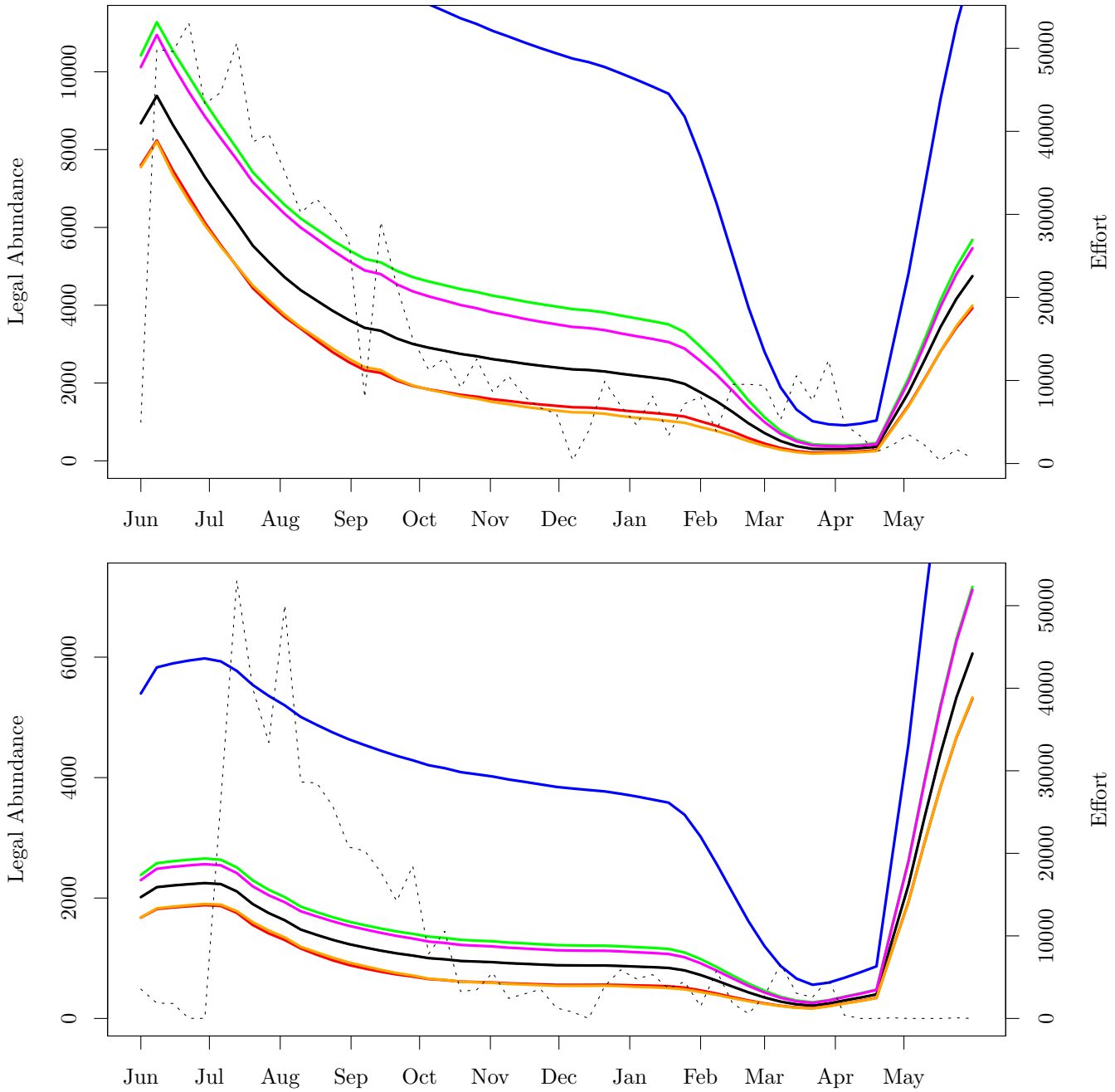

Figure 1.12: Legal population biomass (tonnes) comparison. The years are, from top to bottom, 2004, 2006. The constant, shell, variable, seasonal, effort, temperature driven vulnerability hypotheses are shown in black, blue, green, red, magenta, and orange respectively. On the right y-axis I show the number of traps hauled (dashed lines).

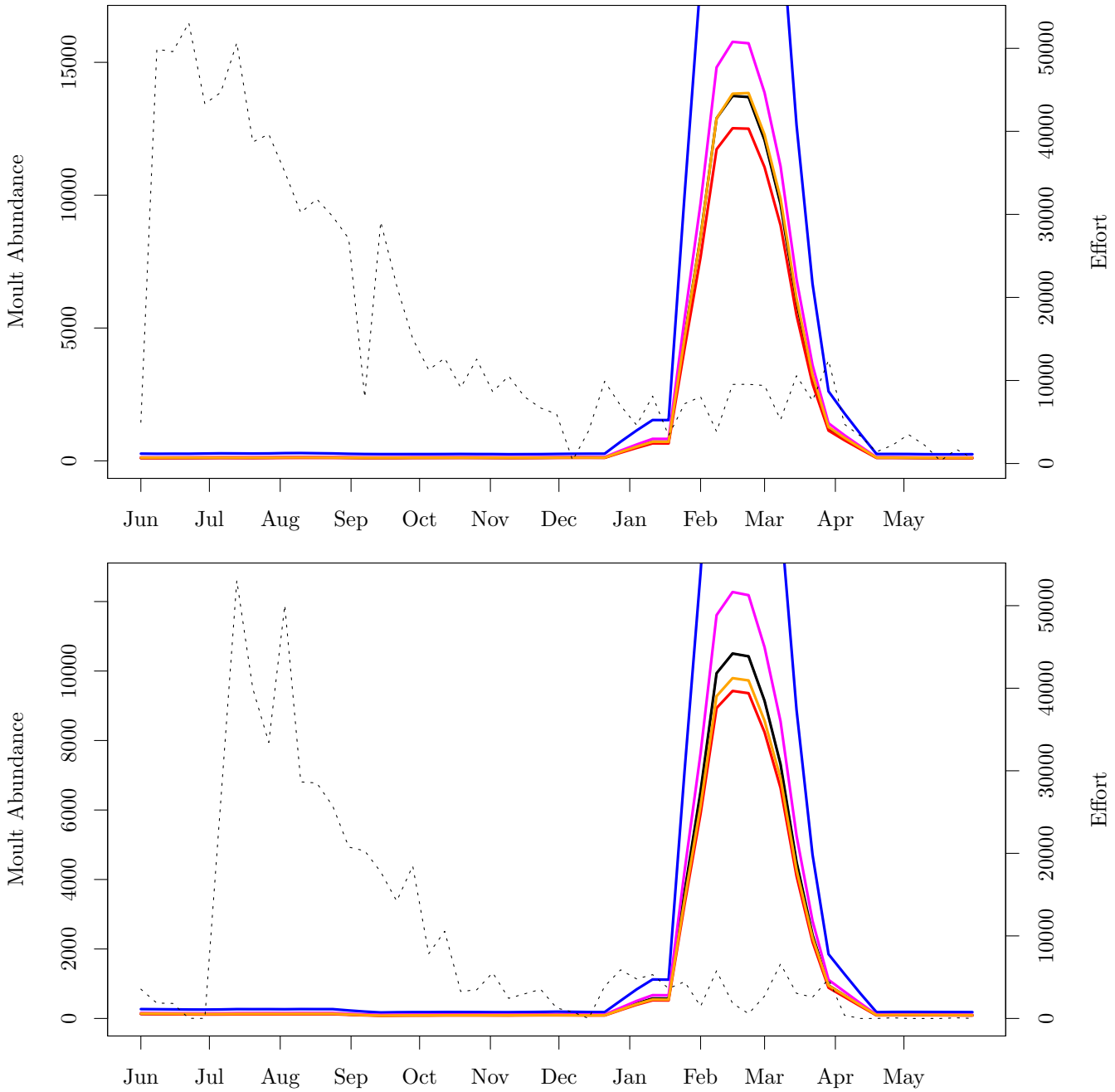

Figure 1.13: Moult comparison. The years are, from top to bottom, 2004, 2006. The constant, shell, variable, seasonal, effort, temperature driven vulnerability hypotheses are shown in black, blue, green, red, magenta, and orange respectively. On the right y-axis I show the number of traps hauled (dashed lines).

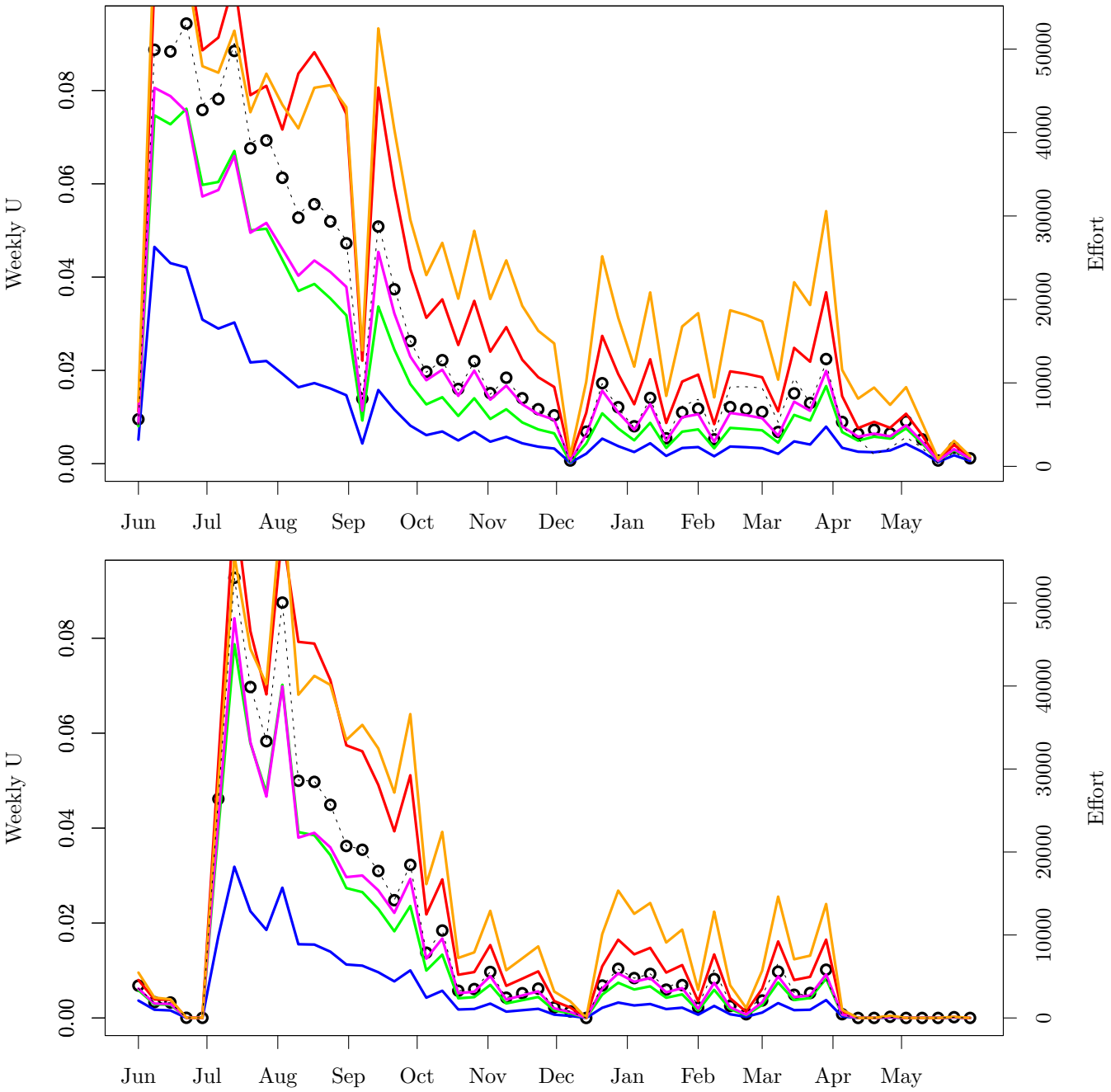

Figure 1.14: Exploitation Rate comparison. The years are, from top to bottom, 2004, 2006. The constant (open circles), shell, variable, seasonal, effort, temperature driven vulnerability hypotheses are shown in black, blue, green, red, magenta, and orange respectively. On the right y-axis I show the number of traps hauled (dashed lines) To make each week clear and avoid blocking out the weekly effort series, the constant scenario is shown as an open circle.

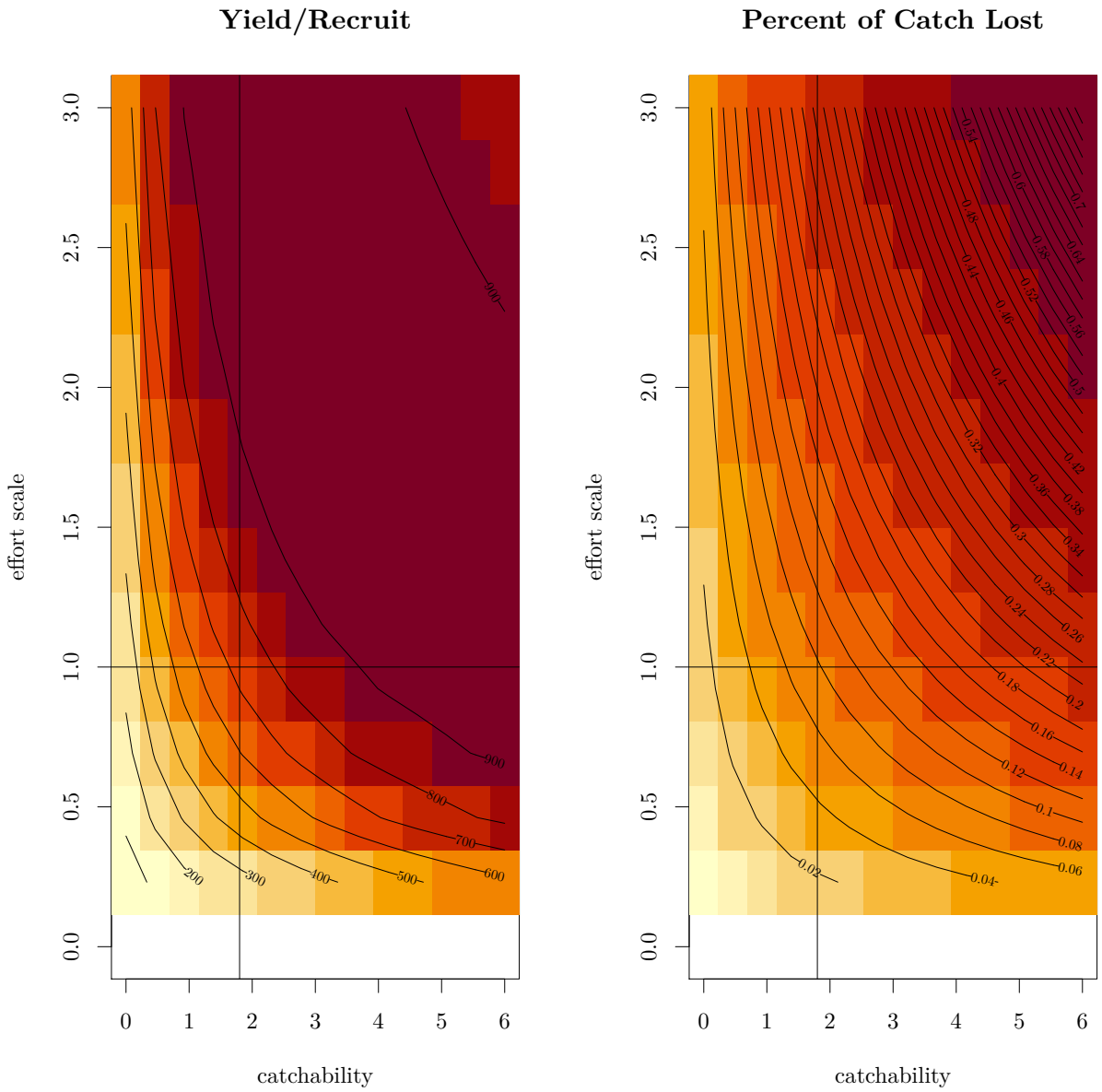

Figure 1.15: Yield per recruit (grams/recruit) under constant vulnerability. The handling mortality (M_h) is set in the figure at $.49wk^{-1}$. M_h is defined in equation 1.7 and is applied on a weekly basis. Note that the mortality on shell condition three increases as a function of catchability and effort scale. It should be noted that the percentage lost is computed according to Equation 1.17, and is not re-scaled by a factor of 100. The vertical line shows the estimated value of catchability. The horizontal line shows where the effort scale is one. The 2003 effort series is used, scaled by the effort scale. When the effort scale is two, there is twice the amount of the weekly fishing effort than was observed in 2003. The effort scale set at one is the unscaled fishing effort series. The intersection of lines shows the observed catchability at the unscaled effort scale; thus, the 2003 yield per recruit (or percentage lost) at the estimated catchability.

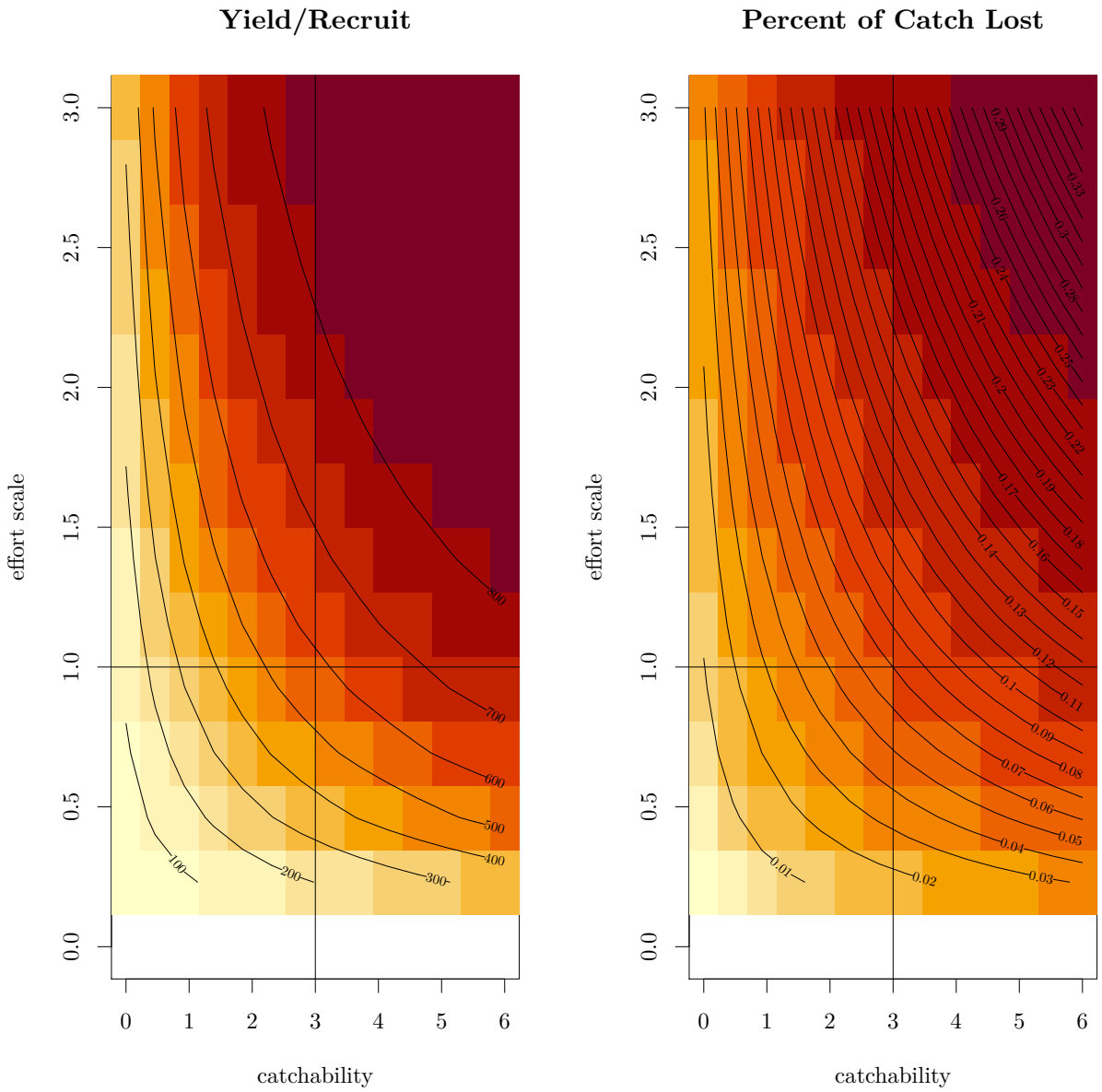

Figure 1.16: Yield per recruit (grams/recruit) under variable vulnerability. The handling mortality (M_h) is set in the figure at $.49wk^{-1}$. M_h is defined in equation 1.7 and is applied on a weekly basis. Note that the mortality on shell condition three increases as a function of catchability and effort scale. It should be noted that the percentage lost is computed according to Equation 1.17, and is not re-scaled by a factor of 100. The vertical line shows the estimated value of catchability. The horizontal line shows where the effort scale is one. The 2003 effort series is used, scaled by the effort scale. When the effort scale is two, there is twice the amount of the weekly fishing effort than was observed in 2003. The effort scale set at one is the unscaled fishing effort series. The intersection of lines shows the observed catchability at the unscaled effort scale; thus, the 2003 yield per recruit (or percentage lost) at the estimated catchability.

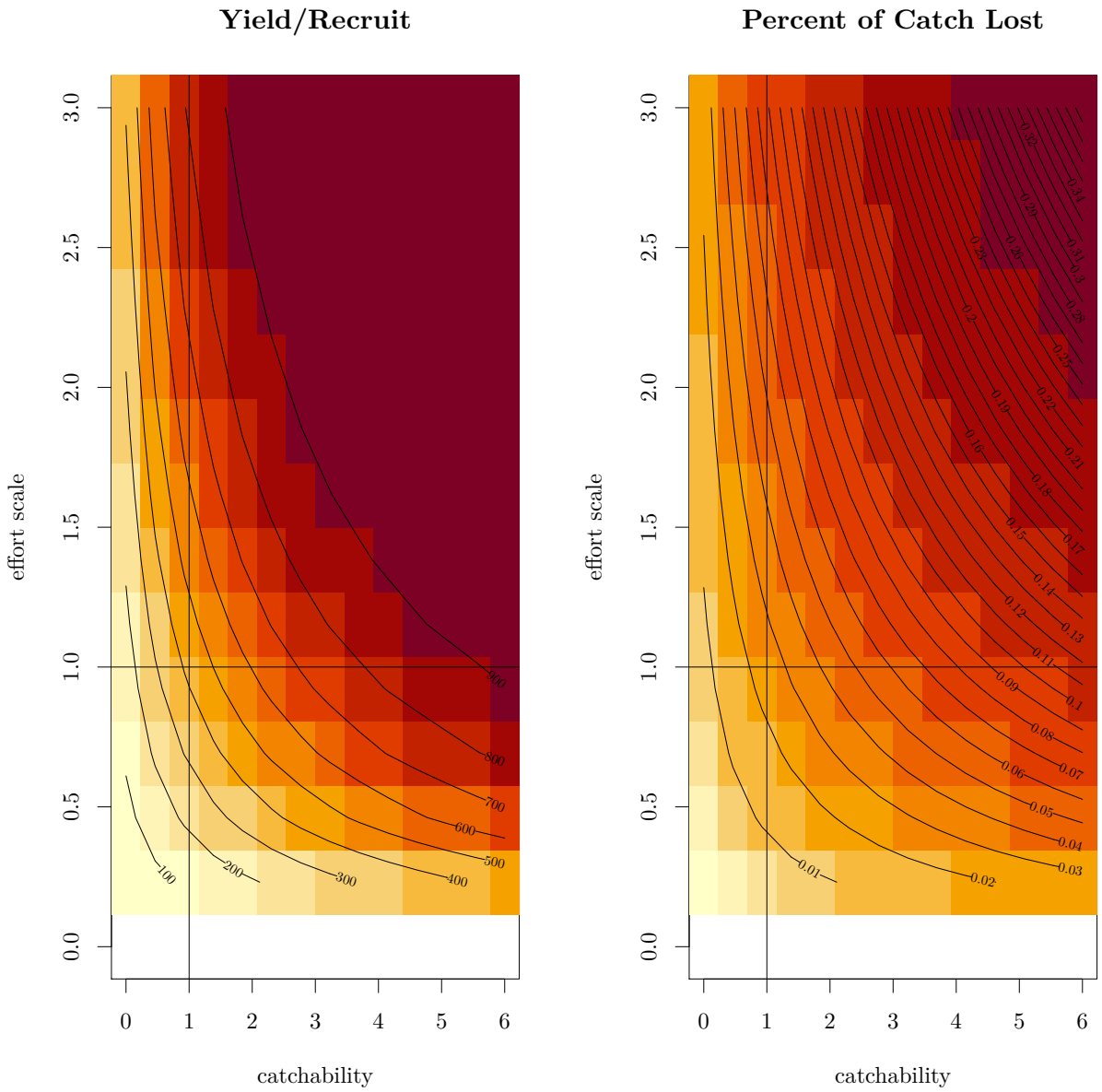

Figure 1.17: Yield per recruit (grams/recruit) under shell vulnerability. The handling mortality (M_h) is set in the figure at $.49wk^{-1}$. M_h is defined in equation 1.7 and is applied on a weekly basis. Note that the mortality on shell condition three increases as a function of catchability and effort scale. It should be noted that the percentage lost is computed according to Equation 1.17, and is not re-scaled by a factor of 100. The vertical line shows the estimated value of catchability. The horizontal line shows where the effort scale is one. The 2003 effort series is used, scaled by the effort scale. When the effort scale is two, there is twice the amount of the weekly fishing effort than was observed in 2003. The effort scale set at one is the unscaled fishing effort series. The intersection of lines shows the observed catchability at the unscaled effort scale; thus, the 2003 yield per recruit (or percentage lost) at the estimated catchability.

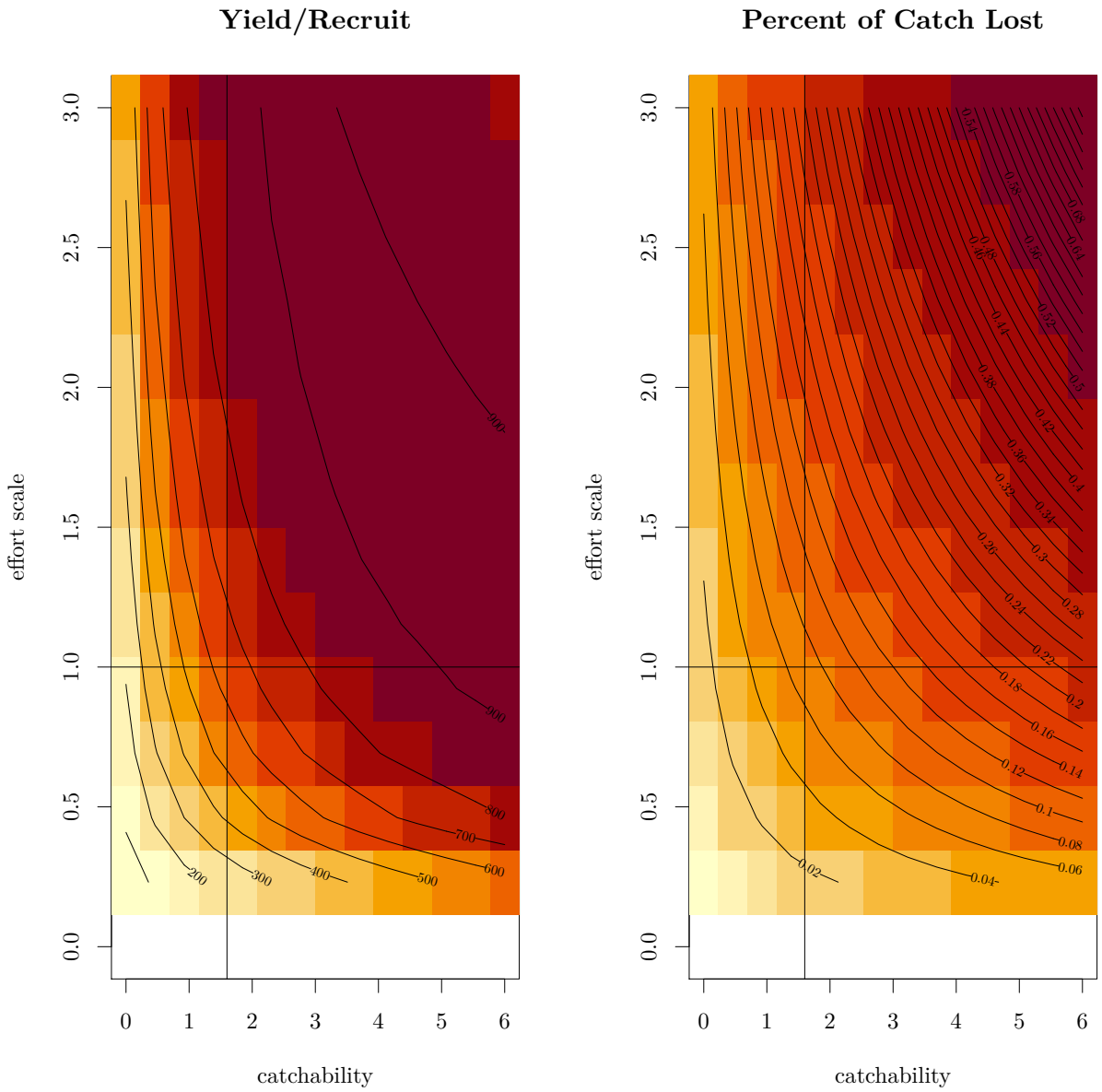

Figure 1.18: Yield per recruit (grams/recruit) under effort vulnerability. The handling mortality (M_h) is set in the figure at $.49wk^{-1}$. M_h is defined in equation 1.7 and is applied on a weekly basis. Note that the mortality on shell condition three increases as a function of catchability and effort scale. It should be noted that the percentage lost is computed according to Equation 1.17, and is not re-scaled by a factor of 100. The vertical line shows the estimated value of catchability. The horizontal line shows where the effort scale is one. The 2003 effort series is used, scaled by the effort scale. When the effort scale is two, there is twice the amount of the weekly fishing effort then was observed in 2003. The effort scale set at one is the unscaled fishing effort series. The intersection of lines shows the observed catchability at the unscaled effort scale; thus, the 2003 yield per recruit (or percentage lost) at the estimated catchability.

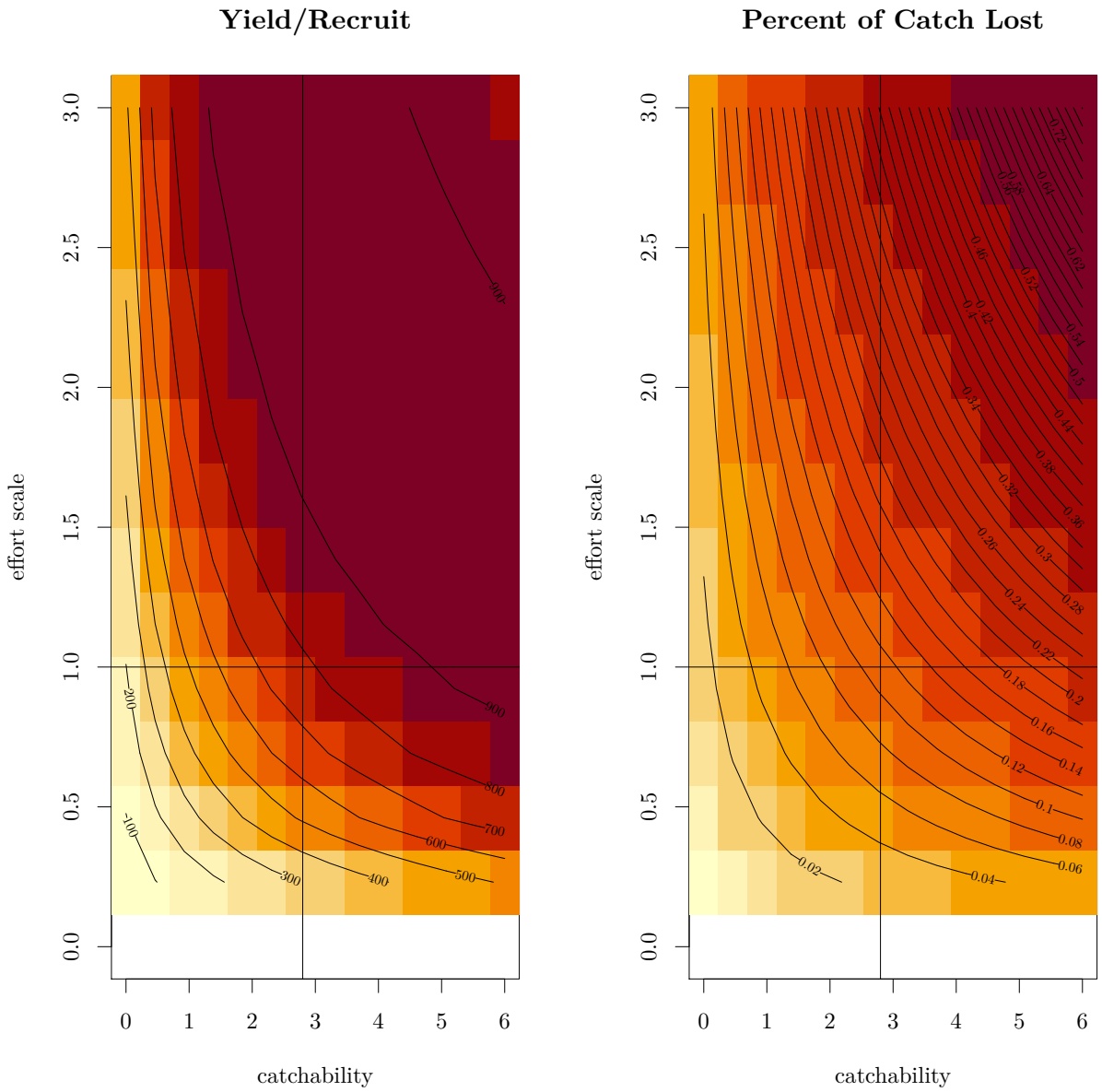

Figure 1.19: Yield per recruit (grams/recruit) under seasonal vulnerability. The handling mortality (M_h) is set in the figure at $.49wk^{-1}$. M_h is defined in equation 1.7 and is applied on a weekly basis. Note that the mortality on shell condition three increases as a function of catchability and effort scale. It should be noted that the percentage lost is computed according to Equation 1.17, and is not re-scaled by a factor of 100. The vertical line shows the estimated value of catchability. The horizontal line shows where the effort scale is one. The 2003 effort series is used, scaled by the effort scale. When the effort scale is two, there is twice the amount of the weekly fishing effort than was observed in 2003. The effort scale set at one is the unscaled fishing effort series. The intersection of lines shows the observed catchability at the unscaled effort scale; thus, the 2003 yield per recruit (or percentage lost) at the estimated catchability.

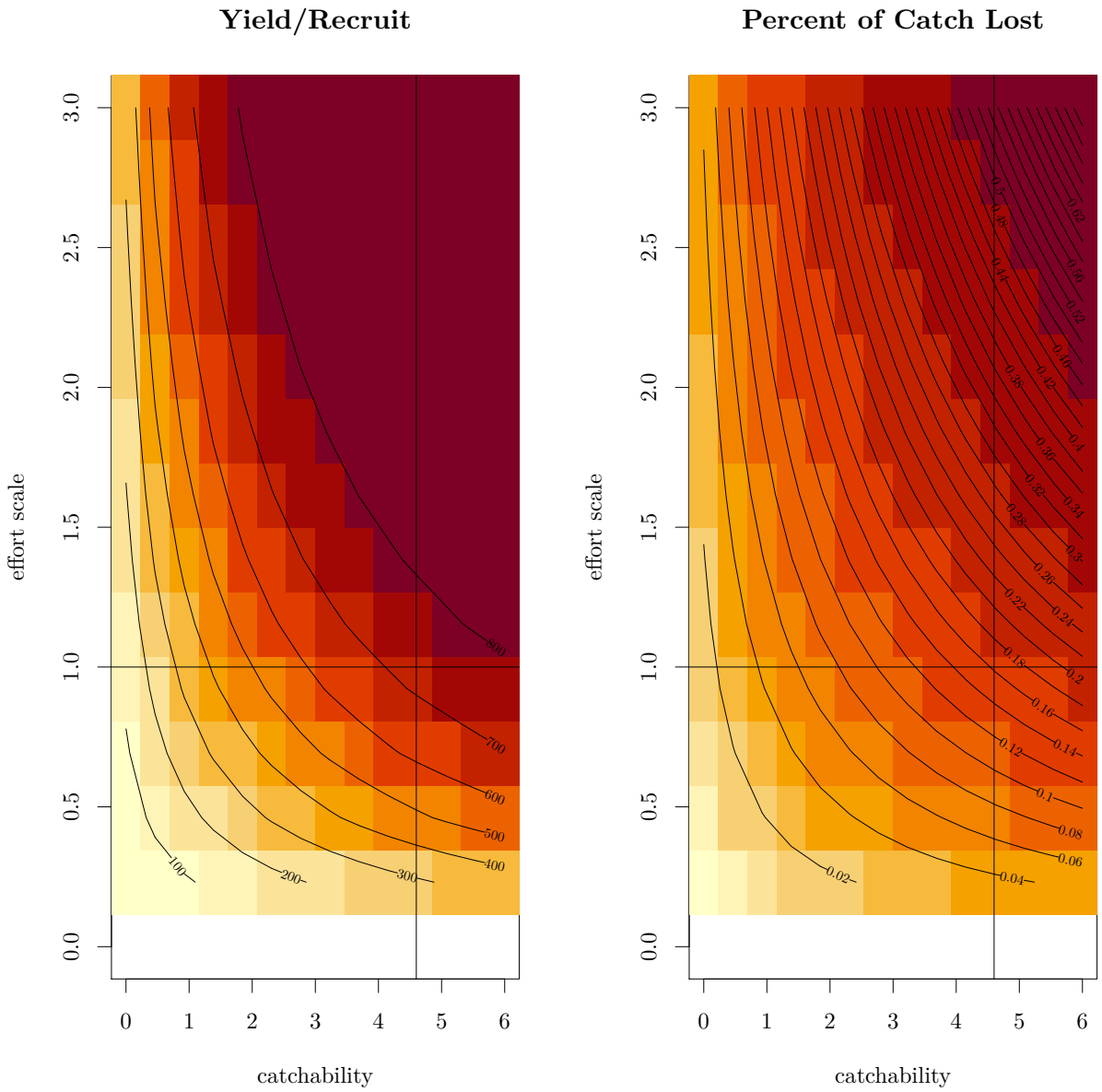

Figure 1.20: Yield per recruit (grams/recruit) under temperature vulnerability. The handling mortality (M_h) is set in the figure at $.49wk^{-1}$. M_h is defined in equation 1.7 and is applied on a weekly basis. Note that the mortality on shell condition three increases as a function of catchability and effort scale. It should be noted that the percentage lost is computed according to Equation 1.17, and is not re-scaled by a factor of 100. The vertical line shows the estimated value of catchability. The horizontal line shows where the effort scale is one. The 2003 effort series is used, scaled by the effort scale. When the effort scale is two, there is twice the amount of the weekly fishing effort then was observed in 2003. The effort scale set at one is the unscaled fishing effort series. The intersection of lines shows the observed catchability at the unscaled effort scale; thus, the 2003 yield per recruit (or percentage lost) at the estimated catchability.

Simulated Vulnerability.	Estimated Vulnerability	Catch Bias	Exp Bias	Exp RMSE	LA Bias	LA RMSE
Constant	Constant	-0.000349	-0.00119	0.00199	0.00103	0.000477
Constant	Variable	-0.000322	-0.00711	0.00211	0.00632	0.000527
Constant	Shell	-0.000728	0.0205	0.00211	-0.0203	0.000907
Constant	Seasonal	-0.000342	-0.00108	0.00208	0.00112	7e-04
Constant	Effort	-0.000349	-0.00119	0.00199	0.00103	0.000477
Constant	Temperature	-0.00089	-0.00336	0.00199	-0.3	0.0973
Variable	Constant	-0.00129	0.361	0.0148	-0.24	0.0107
Variable	Variable	-0.000401	-0.158	0.00774	0.206	0.0102
Variable	Shell	-0.00112	0.349	0.0144	-0.234	0.0104
Variable	Seasonal	-0.000608	0.375	0.0153	-0.245	0.0109
Variable	Effort	-0.00129	0.361	0.0148	-0.24	0.0107
Variable	Temperature	-0.000705	0.419	0.0171	-0.885	0.0405
Shell	Constant	-0.0121	2.23	0.0882	-0.683	0.0302
Shell	Variable	-0.0127	1.18	0.0506	-0.54	0.0238
Shell	Shell	-0.000329	0.0749	0.00361	-0.0706	0.00311
Shell	Seasonal	-0.000755	2.66	0.107	-0.705	0.0311
Shell	Effort	-0.0115	1.94	0.0769	1.2e+24	1.72e+23
Shell	Temperature	0.00985	2.24	0.092	7.06e+104	1.01e+104
Seasonal	Constant	-0.0206	-0.204	0.0105	0.152	0.00688
Seasonal	Variable	-0.0205	-0.462	0.0197	0.658	0.0294
Seasonal	Shell	-0.0136	-0.463	0.0199	0.734	0.0327
Seasonal	Seasonal	-0.00085	-0.0182	0.00211	0.0141	0.000721
Seasonal	Effort	-0.0204	-0.203	0.0104	0.152	0.00685
Seasonal	Temperature	-0.00428	-0.192	0.00873	-0.745	0.0396
Effort	Constant	-0.000428	0.00555	0.00202	-0.00546	0.00046
Effort	Variable	-0.000403	-0.00305	0.00217	0.00183	0.000468
Effort	Shell	-0.000633	0.0187	0.00212	-0.0184	0.000822
Effort	Seasonal	-0.000153	0.0106	0.00211	-0.00919	0.000702
Effort	Effort	-0.000427	0.00555	0.00202	-0.00545	0.000459
Effort	Temperature	-0.000613	0.00905	0.00204	-0.613	0.0753
Temperature	Constant	-0.0718	0.169	0.0115	-0.294	0.0134
Temperature	Variable	-0.0754	-0.274	0.016	0.0861	0.00486
Temperature	Shell	-0.0368	-0.59	0.028	1.07	0.0479
Temperature	Seasonal	-0.029	0.172	0.009	-0.207	0.00935
Temperature	Effort	-0.0719	0.169	0.0115	-0.294	0.0135
Temperature	Temperature	-0.000903	-0.0103	0.00216	0.0067	0.000533

Table 1.16: Simulation evaluation: The table shows the bias for catch, exploitation rate and legal abundance. It also shows the RMSE for exploitation rate and legal abundance. Each row corresponds to a simulation scenario where I simulate data under the Sim vulnerability regime and estimate under the estimated vulnerability regime. The underlined rows correspond to scenarios where the simulated and estimated regimes were the same.

Bibliography

[1] Chiu Chen, John M. Hoenig, Earl G. Dawe, Cavell Brownie, and Kenneth H Pollock. New developments in change-in-ratio and index-removal methods, with application to snow crab (*Chionoecetes opilio). In G.S. Jamieson and A Campbel, editors,* Proceedings of the North Pacific Symposium on Invertebrate Stock Assessment and Management*, volume 125, pages 49–62. NRC-CNRC, 1998.* → *pages 3*

[2] Elizabeth Ann Chilton, Claire E Armistead, and Robert James Foy. The 2010 eastern bering sea continental shelf bottom trawl survey: results for commercial crab species. 2011. → *pages 33*

[3] J.S. Dunham, A. Phillips, J. Morrison, and G Jorgensen. A manual for dungeness crab surveys in british columbia. Technical report, Canadian Technical Report Fisheries Aquatic Science, 2011. → *pages 5*

[4] S.D Frusher, R.B Kennedy, and I.D Gibson. Preliminary estimates of exploitation rates in the tasmanian rock lobster (Jasus edwardsii) fishery using the change-in-ratio and index-removal techniques with tag-recapture data. In G.S. Jamieson and A Campbel, editors, Proceedings of the North Pacific Symposium on Invertebrate Stock Assessment and Management*, volume 125, pages 63–71. NRC-CNRC, 1998.* → *pages 3*

[5] Quentin R. Grafton, Ray Hilborn, Dale Squaires, and Meryl J. Williams. Marine Fisheries Conservation and Management*, chapter 1. Oxford University Press, 2010.* → *pages 35*

[6] Bridget S Green, Caleb Gardner, Jennifer D Hochmuth, and Adrian Linnane. Environmental effects on fished lobsters and crabs. Reviews in Fish Biology and Fisheries*, 24(2):613–638, 2014.* → *pages 34*

[7] R. Donald Gunderson. Surveys of Fisheries Resources*. John Wiley and Sons Inc, 1993.* → *pages 2*

[8] Thomas F. Ihde, Stewart D. Frusher, and John M. Hoenig. Do large rock lobsters inhibit smaller ones from entering traps?: A field experiment. Marine and Freshwater Research*, 57 (7):665–674, 2006. URL* https://doi.org/10.1071/MF05238*.* → *pages 3*

[9] D. W. McLeese and D. G. Wilder. The activity and catchability of the lobster (homarus americanus) in relation to temperature. Journal of the Fisheries Research Board of Canada*, 15(6):1345–1354, 1958.* doi:10.1139/f58-073*. URL* https://doi.org/10.1139/f58-073*.* → *pages 1, 3, 34*

[10] Paul E. McShane. Assessing stocks of abalone (Haliotis spp.):methods and constraints. In Proceedings of the North Pacific Symposium on Invertebrate Stock Assessment and Management*, volume 125, pages 41–49. NRC-CNRC, 1998.* → *pages 3*

[11] *Robert J. Miller. Effectiveness of crab and lobster traps.* Canadian Journal of Fisheries and Aquatic Sciences, *47(6):1228–1251, 1990. doi:10.1139/f90-143. URL https://doi.org/10.1139/f90-143.* → *pages 2, 3*

[12] *Kate Richerson, André E. Punt, and Daniel S. Holland. Nearly a half century of high but sustainable exploitation in the dungeness crab (cancer magister) fishery.* Fisheries Research, *226:105528, 2020. ISSN 0165-7836. doi:https://doi.org/10.1016/j.fishres.2020.105528. URL http://www.sciencedirect.com/science/article/pii/S016578362030045X.* → *pages 33*

[13] *Marianne Robert, Abdelmalek Faraj, Murdoch K. McAllister, and Etinne Rivot. Bayesian State-Space modelling of the De Lury depletion model; strengths and limitations of the method, and application to the Moroccan octopus fishery.* ICES Journal of Marine Science, *67:1272–1290, 2010.* → *pages 3*

[14] *M. John Tremblay and Stephen J. Smith. Lobster (homarus americanus) catchability in different habitats in late spring and early fall.* Marine and Freshwater Research, *52(8):1321–1331, Jan 2002. URL https://doi.org/10.1071/MF01171.* → *pages 3, 20, 53*

[15] *Carl J. Walters and J.D. Martell.* Fisheries Ecology and Management. *Princton University Press, 2004.* → *pages 1, 3, 35*

[16] *Ramzi Yonis. The Economics of British Columbia's Crab Fishery: Socio-economic Profile, Viability, and Market Trends. Technical report, Fisheries and Oceans Canada, 2010.* → *pages 33*

[17] *Z. Zhang, W. Hajas, A. Phillips, and J.A. Boutillier. Evaluation of an intensive fishery on Dungeness crab, Cancer magister, in Fraser Delta, British Columbia. Technical report, Fisheries and Oceans Canada, 2002.* → *pages 7, 8*

[18] *Z. Zhang, W. Hajas, A. Phillips, and J.A. Boutillier. Use of length-based models to estimate biological parameters and conduct yield analyses for male Dungeness Crab (Cancer magister).* Canadian Journal of Fisheries and Aquatic Sciences, *61:2126–2134, November 2004.* → *pages 31*

[19] *Philippe E. Ziegler, Malcolm Haddon, Stewart D. Frusher, and Craig R. Johnson. Modelling seasonal catchability of the southern rock lobster jasus edwardsii by water temperature, moulting, and mating.* Marine Biology, *145(1):179–190, 2004. ISSN 1432-1793. doi:10.1007/s00227-004-1298-6. URL http://dx.doi.org/10.1007/s00227-004-1298-6.* → *pages 2, 3, 34*

.1 Appendix

This appendix shows the results from trying estimate the parameters including natural mortality μ. It focuses on the negative log likelihood, AIC, parameter estimates, and correlation coefficients. Any time-dependent vulnerability hypothesis needs to offer substantial improvements to the fit for it to be worth the extra parameter. It should be noted that there exist some values of α for each vulnerability hypothesis such that the vulnerability hypothesis reduces to the constant vulnerability

hypothesis. Under the variable, temperature, and effort vulnerability hypothesis the model becomes the constant vulnerability hypothesis when α is equal to zero. The seasonal vulnerability hypothesis becomes the constant vulnerability hypothesis when α is equal to one. In Table 17 I show the number of parameters, NLL, AIC, and the depletion and size composition components of the deviance. Most of the difference between the scenarios is in how well they fit the observed catches.

All of the time-dependent vulnerability hypotheses had lower AIC's than the time-independent vulnerability hypotheses. Furthermore, it should be noted that the best-fitting vulnerability hypotheses were the temperature and shell condition hypotheses. This is consistent with several other crustacean fisheries [14].

Vulnerability	Number of Parameters	NLL	Catch Component	Size Component	AIC	Δ AIC
Constant	8	7856	6040	1817	15720	128
Var	9	7853	6034	1819	15714	122
Seasonal	9	7834	6018	1816	15676	84
Effort	9	7824	6008	1817	15656	64
Shell	9	7816	5998	1818	15640	48
Temperature	9	7792	5980	1813	15592	0

Table 17: This table shows the scenario, the number of parameters, and the associated AIC. The scenario with the lowest AIC was the temperature dependent vulnerability scenario.

	Const	Var	Shell	Seasonal	Effort	Temp
N1	0.27 , 0.52 , 0.88	0.33 , 0.65 , 1.2	0.41 , 0.88 , 1.6	0.27 , 0.52 , 0.88	0.37 , 0.71 , 1.2	0.49 , 0.93 , 1.6
N2	0.39 , 0.72 , 1.3	0.47 , 0.92 , 1.6	0.62 , 1.4 , 2.6	0.36 , 0.7 , 1.2	0.53 , 1 , 1.7	0.61 , 1.2 , 2
N3	0.2 , 0.39 , 0.68	0.25 , 0.5 , 0.9	0.43 , 1 , 2	0.18 , 0.35 , 0.6	0.28 , 0.54 , 0.95	0.31 , 0.6 , 1
N4	0.072 , 0.14 , 0.24	0.09 , 0.18 , 0.31	0.16 , 0.37 , 0.72	0.065 , 0.12 , 0.21	0.098 , 0.19 , 0.32	0.11 , 0.21 , 0.35
N5	0.24 , 0.46 , 0.8	0.3 , 0.58 , 1	0.41 , 0.91 , 1.7	0.23 , 0.43 , 0.73	0.34 , 0.64 , 1.1	0.36 , 0.69 , 1.2
q	1.6 , 1.8 , 1.9	2.7 , 3 , 3.4	0.68 , 1 , 1.4	2.4 , 2.8 , 3.2	1.4 , 1.6 , 1.7	4.1 , 4.6 , 5.2
μ	8.5 , 11 , 13	8.9 , 11 , 14	8.7 , 11 , 13	8.4 , 11 , 13	9.3 , 11 , 14	9.8 , 12 , 14
ν	0.16 , 0.17 , 0.19	0.16 , 0.17 , 0.19	0.16 , 0.18 , 0.2	0.16 , 0.17 , 0.19	0.16 , 0.18 , 0.2	0.16 , 0.18 , 0.2
α	1 , 1 , 1	1 , 1.6 , 2.2	0.45 , 0.53 , 0.6	0.68 , 0.74 , 0.8	-0.32 , -0.26 , -0.2	-0.095 , -0.089 , -0.082

Table 18: Parameter Estimates and 95% Confidence Intervals for the estimated parameters N_1, N_2, N_3, N_4, N_5, q, μ, ν and α different vulnerability scenarios. (Lower CI, Mean, Upper CI%)

	Const	Var	Shell	Seasonal	Effort	Temp
N1	0.35 , 0.52 , 0.8	0.44 , 0.64 , 1	0.41 , 0.6 , 0.92	0.36 , 0.54 , 0.84	0.48 , 0.68 , 1.1	0.45 , 0.65 , 1
N2	0.5 , 0.75 , 1.2	0.59 , 0.91 , 1.5	0.6 , 0.88 , 1.4	0.52 , 0.74 , 1.2	0.66 , 0.97 , 1.5	0.6 , 0.85 , 1.3
N3	0.29 , 0.41 , 0.65	0.32 , 0.49 , 0.83	0.35 , 0.55 , 0.93	0.28 , 0.38 , 0.57	0.36 , 0.53 , 0.86	0.29 , 0.45 , 0.72
N4	0.088 , 0.13 , 0.19	0.13 , 0.17 , 0.24	0.12 , 0.18 , 0.26	0.081 , 0.12 , 0.19	0.11 , 0.17 , 0.25	0.092 , 0.14 , 0.22
N5	0.33 , 0.48 , 0.76	0.38 , 0.58 , 0.94	0.39 , 0.57 , 0.92	0.32 , 0.46 , 0.72	0.43 , 0.63 , 0.98	0.36 , 0.52 , 0.81
q	1.5 , 1.7 , 1.8	2.7 , 2.9 , 3.1	1.2 , 1.4 , 1.5	2.4 , 2.6 , 2.9	1.4 , 1.5 , 1.5	3.8 , 4.1 , 4.6
μ	9.6 , 11 , 13	9.9 , 11 , 14	9.7 , 11 , 13	9.7 , 11 , 13	9.9 , 11 , 14	9.7 , 11 , 13
ν	0.17 , 0.18 , 0.2	0.16 , 0.18 , 0.2	0.17 , 0.19 , 0.2	0.17 , 0.18 , 0.21	0.16 , 0.17 , 0.18	0.17 , 0.19 , 0.21
α	1 , 1 , 1	1.1 , 1.4 , 1.7	0.8 , 0.83 , 0.88	0.69 , 0.74 , 0.77	-0.29 , -0.24 , -0.21	-0.092 , -0.085 , -0.08

Table 19: Parameter Estimates and 95% Confidence Intervals for the estimated parameters N_1, N_2, N_3, N_4, N_5, q, μ, ν and α different vulnerability scenarios under constant moult (Lower CI, Mean, Upper CI). Parameters are estimated using the draws from a multivariate normal using the estimated covariance matrix.

Const	N1	N2	N3	N4	N5	q	s	μ
N1	1.00	1.00	0.99	0.95	0.99	-0.35	0.64	0.99
N2	1.00	1.00	0.99	0.95	1.00	-0.37	0.66	1.00
N3	0.99	0.99	1.00	0.95	0.99	-0.38	0.65	0.99
N4	0.95	0.95	0.95	1.00	0.95	-0.37	0.62	0.95
N5	0.99	1.00	0.99	0.95	1.00	-0.38	0.65	0.99
q	-0.35	-0.37	-0.38	-0.37	-0.38	1.00	-0.20	-0.30
ν	0.64	0.66	0.65	0.62	0.65	-0.20	1.00	0.65
μ	0.99	1.00	0.99	0.95	0.99	-0.30	0.65	1.00

Shell	N1	N2	N3	N4	N5	q	s	μ	α_{sh}
N1	1.00	1.00	0.99	0.97	1.00	-0.65	0.61	0.91	-0.44
N2	1.00	1.00	0.99	0.98	1.00	-0.67	0.61	0.90	-0.47
N3	0.99	0.99	1.00	0.98	0.99	-0.72	0.59	0.86	-0.53
N4	0.97	0.98	0.98	1.00	0.98	-0.72	0.58	0.83	-0.54
N5	1.00	1.00	0.99	0.98	1.00	-0.68	0.61	0.89	-0.48
q	-0.65	-0.67	-0.72	-0.72	-0.68	1.00	-0.23	-0.28	0.85
ν	0.61	0.61	0.59	0.58	0.61	-0.23	1.00	0.65	-0.11
μ	0.91	0.90	0.86	0.83	0.89	-0.28	0.65	1.00	-0.08
α_{sh}	-0.44	-0.47	-0.53	-0.54	-0.48	0.85	-0.11	-0.08	1.00

Effort	N1	N2	N3	N4	N5	q	s	μ	α_e
N1	1.00	1.00	0.99	0.96	1.00	-0.49	0.63	0.99	-0.19
N2	1.00	1.00	0.99	0.96	1.00	-0.50	0.65	0.99	-0.20
N3	0.99	0.99	1.00	0.96	0.99	-0.51	0.64	0.99	-0.19
N4	0.96	0.96	0.96	1.00	0.96	-0.49	0.62	0.96	-0.18
N5	1.00	1.00	0.99	0.96	1.00	-0.51	0.64	0.99	-0.20
q	-0.49	-0.50	-0.51	-0.49	-0.51	1.00	-0.27	-0.42	0.32
ν	0.63	0.65	0.64	0.62	0.64	-0.27	1.00	0.65	-0.09
μ	0.99	0.99	0.99	0.96	0.99	-0.42	0.65	1.00	-0.14
α_e	-0.19	-0.20	-0.19	-0.18	-0.20	0.32	-0.09	-0.14	1.00

Var	N1	N2	N3	N4	N5	q	s	μ	α_v
N1	1.00	1.00	0.99	0.95	0.99	-0.15	0.62	0.97	0.30
N2	1.00	1.00	0.99	0.95	1.00	-0.16	0.63	0.97	0.31
N3	0.99	0.99	1.00	0.95	0.99	-0.18	0.63	0.97	0.30
N4	0.95	0.95	0.95	1.00	0.95	-0.17	0.60	0.93	0.29
N5	0.99	1.00	0.99	0.95	1.00	-0.17	0.63	0.97	0.30
q	-0.15	-0.16	-0.18	-0.17	-0.17	1.00	-0.17	-0.22	0.49
ν	0.62	0.63	0.63	0.60	0.63	-0.17	1.00	0.65	0.02
μ	0.97	0.97	0.97	0.93	0.97	-0.22	0.65	1.00	0.10
α_v	0.30	0.31	0.30	0.29	0.30	0.49	0.02	0.10	1.00

Season	N1	N2	N3	N4	N5	q	s	μ	α_{se}
N1	1.00	1.00	0.99	0.95	0.99	-0.13	0.65	1.00	-0.04
N2	1.00	1.00	0.99	0.96	1.00	-0.15	0.66	1.00	-0.02
N3	0.99	0.99	1.00	0.95	0.99	-0.19	0.66	0.99	0.01
N4	0.95	0.96	0.95	1.00	0.96	-0.18	0.63	0.96	0.02
N5	0.99	1.00	0.99	0.96	1.00	-0.17	0.66	1.00	-0.01
q	-0.13	-0.15	-0.19	-0.18	-0.17	1.00	-0.08	-0.14	-0.89
ν	0.65	0.66	0.66	0.63	0.66	-0.08	1.00	0.66	-0.02
μ	1.00	1.00	0.99	0.96	1.00	-0.14	0.66	1.00	-0.02
α_{se}	-0.04	-0.02	0.01	0.02	-0.01	-0.89	-0.02	-0.02	1.00

Temp	N1	N2	N3	N4	N5	q	s	μ	α_t
N1	1.00	1.00	0.99	0.96	0.99	-0.06	0.65	0.99	-0.15
N2	1.00	1.00	1.00	0.97	1.00	-0.09	0.66	1.00	-0.12
N3	0.99	1.00	1.00	0.96	1.00	-0.11	0.66	1.00	-0.10
N4	0.96	0.97	0.96	1.00	0.97	-0.12	0.64	0.97	-0.09
N5	0.99	1.00	1.00	0.97	1.00	-0.12	0.66	1.00	-0.09
q	-0.06	-0.09	-0.11	-0.12	-0.12	1.00	-0.07	-0.13	-0.91
ν	0.65	0.66	0.66	0.64	0.66	-0.07	1.00	0.66	-0.06
μ	0.99	1.00	1.00	0.97	1.00	-0.13	0.66	1.00	-0.07
α_t	-0.15	-0.12	-0.10	-0.09	-0.09	-0.91	-0.06	-0.07	1.00

Table 20: Parameter correlation matrix for the different vulnerability hypothesis. The vulnerability hypothesis is in the upper left corner. Note that the abundance is strongly correlated with natural mortality. Also note that q and σ are often strongly correlated. Estimated from the Hessian